Robust Spatial Confounding Adjustment via Basis Voting

Anik Burman, Elizabeth L. Ogburn*, Abhirup Datta* Department of Biostatistics, Johns Hopkins University

Abstract

Estimating causal effects of spatially structured exposures is complicated by unmeasured spatial confounders, which undermine identifiability in spatial linear regression models unless structural assumptions are imposed. We develop a general framework for causal effect estimation that relaxes the commonly assumed requirement that exposures contain higher-frequency variation than confounders. We propose basis voting, a plurality-rule estimator — novel in the spatial literature — that consistently identifies causal effects only under the assumption that, in a spatial basis expansion of the exposure and confounder, there exist several basis functions in the support of the exposure but not the confounder. This assumption generalizes existing assumptions of differential basis support used for identification of the causal effect under spatial confounding, and does not require prior knowledge of which basis functions satisfy this support condition. We also show that the standard projectionbased estimator used in other methods relying on differential support is inefficient, and provide a more efficient novel estimator. Extensive simulations and a real-world application demonstrate that our approach reliably recovers unbiased causal estimates whenever exposure and confounder signals are separable on a plurality of basis functions. Importantly, by not relying on higher-frequency variation, our method remains applicable to settings where exposures are smooth spatial functions, such as distance to pollution sources or major roadways, common in environmental studies.

Keywords: spatial statistics; geostatistics; plurality rule; mode estimation; kernel density; environmental exposures

^{*}Address for correspondence: eogburn@jhu.edu; abhidatta@jhu.edu

1 Introduction

Estimating the true association between spatially structured exposures and outcomes is a fundamental problem in spatial statistics and environmental epidemiology. However, this task is challenging in the presence of unmeasured spatial variables that simultaneously influence both the exposure and the outcome. When such variables are not accounted for, the (conditional) effect size in standard regression models applied to point-referenced spatial data is unidentifiable, leading to biased estimates. This phenomenon is referred to as *spatial confounding*, and it arises frequently in real-world applications where spatial structure is intrinsic to both the predictors (exposures) and to unmeasured background processes.

An early formal recognition of this issue can be found in Clayton et al. (1993), which demonstrated how including spatially varying error terms in the model changes covariate effect estimates, but this change was favored over the unadjusted estimate which is biased under confounding. Subsequent works have had differing opinions about this (Woodard et al. 1999, Reich et al. 2006, Wakefield 2007, Hodges & Reich 2010, Schnell & Papadogeorgou 2020, Khan & Calder 2022, Zimmerman & Ver Hoef 2022) with arguments put forth both for and against including spatially correlated errors in the model. A particularly influential contribution by Paciorek (2010) quantified this bias in generalized least squares (GLS) settings, relating it to the relative smoothness of the exposure and the unmeasured confounder. This work also underscored the identifiability challenges of separating the exposure effect from the influence of spatial confounding, unless certain restrictions or structural assumptions are imposed. Extensive theoretical and empirical results in Khan & Berrett (2023) largely agree with the conclusions of Paciorek (2010). Related work in spatial prediction frameworks, such as that of Page et al. (2017), arrives at similar conclusions. Gilbert et al. (2025) proved that the GLS estimator is consistent under varied forms of spatial confound-

ing as long as the exposure has some non-spatial variation. Dupont et al. (2022) proves consistency of their spatial+ method under a similar assumption of Gaussian noise in the exposure. Gilbert et al. (2021) grounded the spatial confounding problem in the framework of causal inference, going beyond the linear regression case. Their sufficient conditions for identifiability of a causal effect under confounding also assumed some non-spatial variation in the exposure.

Things get more complicated if the exposure is only a function of space with no non-spatial component. Such examples are common in many environmental studies, e.g., studying the effect of distance to fracking mines on health (Casey et al. 2016, Currie et al. 2017) or of distances to roadways on air-quality (Karner et al. 2010). Brugge et al. (2013) explicitly raises concerns about the inability to adjust for co-smooth spatial confounders. Estimators like GLS and spatial+ whose consistency is guaranteed in the presence of noise in the exposure, may no longer work in this smooth-exposure setting. In fact, it has been proven that when exposures are too smooth relative to the confounder, the exposure effect cannot be identified even in a linear regression setting (Bolin & Wallin 2024, Datta & Stein 2025). In the setting of smooth exposures, most methods rely on the assumption that confounders vary mainly at broad spatial scales, while exposures may display more localized, highfrequency spatial patterns. Extensive experiments Paciorek (2010) and Khan & Berrett (2023) have shown that such a situation is favorable for recovery of the exposure effect as the exposure becomes unconfounded at higher frequencies. This, along with the assumption of a linear relationship between the outcome and the exposure, common in spatial setup, solves the problem of spatial confounding. Methods that build on this idea include both parametric and semi-parametric approaches, such as those proposed in Thaden & Kneib (2018), Keller & Szpiro (2020), Dupont et al. (2022), and Guan et al. (2023).

When the unmeasured confounder has the same or finer spatial variation than the exposure,

existing techniques generally fail, and standard spatial estimators can perform worse than even the unadjusted estimator as seen in Paciorek (2010), Khan & Berrett (2023). This can be viewed through the lens of causal inference as a violation of the positivity assumption, which requires that all levels of exposure be observed across levels of confounders. Nonetheless, there are important cases where this assumption does not hold. As mentioned earlier, spatial contours of exposures like distances to industrial sites, greenery, or major roadways can be quite smooth, precluding the use of techniques relying on presence of high-frequency variation unique to the exposure. In fact, the notion of smoothness defined by the ordering of basis functions may not generalize to two or higher-dimensional spatial domains. For example, using kronecker product of basis functions of one-dimensional basis, creates a two-dimensional basis with two indices dictating smoothness (one along each coordinate). Approaches like those of Keller & Szpiro (2020) which model the confounder using basis functions of low-indices do not easily generalize for such basis sets.

In this work, we develop a general framework for effect estimation in the spatial linear regression model that adjusts for unmeasured spatial confounders, without assuming that the confounders are smoother than the exposure. Instead, we introduce a milder plurality rule assumption, inspired by ideas in the robust instrumental variable (IV) literature. The central assumption is that, in a representation of the exposure X and the confounder U along a set of orthonormal basis functions, the set of ratios of the projections of U and X on each of the basis functions has a larger cluster around zero than around any other value. This assumption subsumes the rougher exposure assumption as a special case. Under plurality, we show that a set of candidate estimators of the regression effect, one based on each basis function, will have the mode around the true coefficient value. We prove that this enables consistent estimation of the effect forgoing the requirement of prior knowledge of which basis functions support only the exposure. We call the method basis voting, as

each basis yields a candidate estimate, and the most popular candidate (mode) is the final estimate.

A second contribution is improving the choice of the candidate estimator. Plurality rule based deconfounding has recently been considered for time-series data (Schur & Peters 2024), and the candidate estimator used is the ratio of the projections of the outcome and the exposure along a basis function. We show that this estimator is inefficient, and present a better candidate estimator with lower asymptotic variance and finite-sample unbiasedness. We provide consistency and asymptotic normality of a plurality of the candidate estimators and consistency of the aggregate mode estimator based on the candidates. We empirically demonstrate robustness to the choice of basis functions used for analyzing the data.

The remainder of the paper is organized as follows. Section 2 introduces the data-generating mechanism and formalizes the identifiability challenges. Section 3 presents the proposed basis voting estimator using basis function expansions. Section 4 describes competing methods for constructing candidate estimators and analyzes their properties in large samples. Section 5 reports results from a comprehensive simulation study comparing our method to existing approaches. Section 6 showcases an empirical analysis of county-level COVID-19 mortality and air pollution, illustrating the practical implementation and utility of the proposed method. Finally, Section 7 concludes with a discussion of the implications of our findings and directions for future work.

2 Problem Setup and Assumptions

Let $\mathcal{D} \subseteq \mathbb{R}^d$ denote a compact spatial domain, and let $\mathbf{S}_n = \{S_1, \dots, S_n\}$ represent n spatial locations sampled from a distribution with density $f_S(\cdot)$ on \mathcal{D} . At each location S_i , we observe an exposure value $X_i := X(S_i)$ and an outcome value $Y_i := Y(S_i)$. We denote the exposure and outcome vectors by $\mathbf{X}_n = (X_1, \dots, X_n)^{\top}$ and $\mathbf{Y}_n = (Y_1, \dots, Y_n)^{\top}$,

respectively. In addition to X and Y, we assume there exists an unmeasured confounder U defined at each location, $U_i := U(S_i)$, represented by the vector $\mathbf{U}_n = (U_1, \dots, U_n)^{\mathsf{T}}$, which is correlated with the exposure and affects the outcome. Both the exposure and the unmeasured confounder are assumed to be univariate.

In keeping with the spatial statistics literature, we assume throughout a linear data generating process (DGP) for the outcome at a generic spatial location $s \in \mathcal{D}$:

$$Y(s) = \beta X(s) + U(s) + \epsilon(s), \tag{1}$$

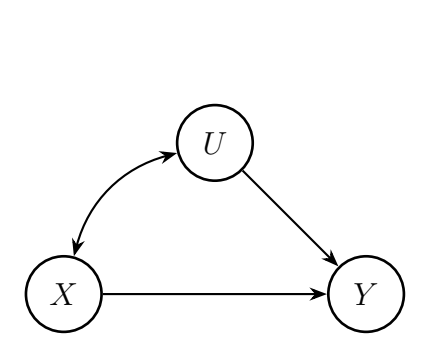
where β is the exposure effect of interest, $\epsilon(s)$ is an independent mean-zero error term, and U(s) is collinear with X(s). If the confounder U were measured, then it would be straightforward to estimate the exposure effect β , simply by regressing Y in X and U and looking at the estimated slope for X. As U is not measured, we cannot directly adjust for it in the model. In this paper, we propose novel assumptions under which we can estimate the true causal effect β in the presence of the unmeasured confounding by U.

We will be assuming that both X and U are deterministic (fixed) functions of space, in $\mathcal{L}^4(\mathcal{D}, f_S)$, the Hilbert space of all fourth-power integrable functions with respect to the sampling measure f_S with the inner product induced by it denoted by $\langle g, h \rangle_{f_S} := \int_{\mathcal{D}} g(s)h(s)f_S(s)ds$ and the corresponding norm $\|\cdot\|_{f_S}$. Let $\mathcal{H} = \{h_1, h_2, \cdots\}$ denote an infinite-dimensional orthonormal basis of $\mathcal{L}^4(\mathcal{D}, f_S)$. Unlike prior approaches, our method does not require an assumption that the basis functions h_1, h_2, \cdots are ordered by their degree of smoothness or roughness, with X having a longer expansion than U.

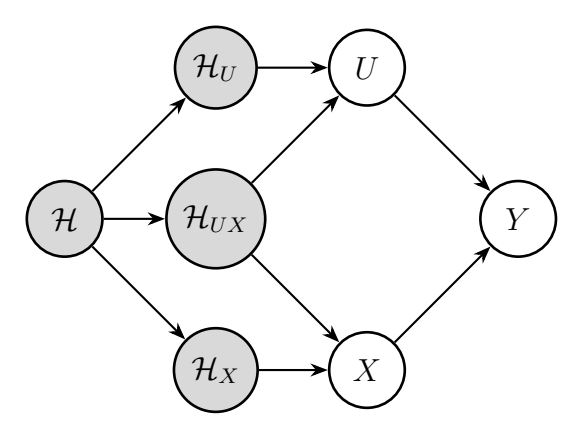
Let $X(s) = \sum_{j=1}^{\infty} \alpha_x^{(j)} h_j(s)$ and $U(s) = \sum_{j=1}^{\infty} \alpha_u^{(j)} h_j(s)$ with finite L^2 norms: $\mathbb{E}[X(S)]^2 = \sum_j \left|\alpha_x^{(j)}\right|^2 < \infty$ and $\mathbb{E}[U(S)]^2 = \sum_j \left|\alpha_u^{(j)}\right|^2 < \infty$. By orthogonality, the projections of X on each of the basis functions are given by the coefficients $\alpha_x^{(j)} = \langle X, h_j \rangle_{f_S}$ and similarly for $\alpha_u^{(j)}$. Because X and U are square-integrable, for any $\epsilon > 0$, there exists $d := d(\epsilon) \in \mathbb{N}$ large enough such that $\max\left\{\|X_{>d}\|_{f_S}^2, \|U_{>d}\|_{f_S}^2\right\} < \epsilon$, where $\|f_{>d}\|_{f_S}$ is the norm of the

residual of the function f after projecting it on the first d basis functions. In other words, the expansion of X and U with respect to h_1, h_2, \dots, h_d is a good approximation (X, U).

Without loss of generality, we partition \mathcal{H} into three disjoint sets $\mathcal{H} = \mathcal{H}_{UX} \sqcup \mathcal{H}_{X} \sqcup \mathcal{H}_{U}$ where \mathcal{H}_{UX} is the set of basis functions shared by both U and X, \mathcal{H}_{X} is the set unique to X and similarly for \mathcal{H}_{U} . Figure 1 depicts our DGP, with and without basis expansion. If



(a) Standard confounding setting with bidirectional link between U and X



(b) Expanded setting with basis components (shaded grey)

Figure 1: Two graphical representations of the data-generating mechanism: (a) standard confounding and (b) the expanded graph, which shows the basis representation.

 $\mathcal{H}_{UX} = \emptyset$, where \emptyset is the null set, then U is orthogonal to X and does not confound the effect of X on Y. We therefore focus on the setting where \mathcal{H}_{UX} is nonempty, representing nontrivial confounding. It may be the case that $\mathcal{H}_U = \emptyset$, implying that the confounder does not have any independent variation, but we must have $\mathcal{H}_X \neq \emptyset$ because if not, it is not possible to extract the independent effect of X on Y and thus β is unidentifiable. Let us formalize this identification assumption:

Assumption 1 (Direction of No Confounding). Let $\alpha_x = (\alpha_x^{(1)}, \alpha_x^{(2)}, \dots)$ and $\alpha_u = (\alpha_u^{(1)}, \alpha_u^{(2)}, \dots)$ be the sequence of coefficients of X and U for the basis function set \mathcal{H} respectively, then there exists a non-empty subset $O_X \subseteq \{1, \dots, d\}$ such that for all $j \in O_X$, we have $\alpha_u^{(j)} = 0$ and $\alpha_x^{(j)} \neq 0$ where $d \in \mathbb{N}$ with $\max \{\|X_{>d}\|_{f_S}^2, \|U_{>d}\|_{f_S}^2\} < \epsilon$ for some

small $\epsilon > 0$.

If the index j of even a single basis function $h_j \in O_X$ were known, h_j would suffice to identify β . This is because the effect of h_j itself on Y is unconfounded, and under linearity, its effect is equal to β . In practice, however, this will never be the case as O_X is unknown. Previous methods, e.g., Keller & Szpiro (2020), have instead relied on the assumption that the highest frequency basis functions are unconfounded, i.e., essentially they assume that the basis functions are ordered in terms of increasing roughness or frequency $h_1 \lessapprox h_2 \lessapprox \cdots \lessapprox h_d$, and there exists some $t \le d \in \mathbb{N}$ such that $\{t+1,\cdots,d\} \in O_X$. So, Assumption 1 is strictly weaker as, rather than requiring unconfounded high-frequency components, we only assume the existence of a non-trivial set $\{h_j: j \in O_X\}$. This formulation accommodates cases where the unconfounded variation in X lies at low or intermediate spatial scales. Figure 2 shows two such scenarios where the roughness ordering of X and U is different and still can be framed by our formulation. This also broadens the scope for the choice of basis functions used for analysis, as we can now use basis functions that might not have a canonical ordering of roughness, like basis functions on multivariate domains \mathbb{R}^d generated as a Kronecker product of bases on \mathbb{R} .

A helpful way to interpret the subset of basis functions $\{h_j : j \in O_X\}$ is through the lens of instrumental variable (IV) methods in causal inference. In classical IV frameworks, one seeks an instrument Z that satisfies two key properties: (i) it is correlated with the exposure X, and (ii) it is independent of the unmeasured confounder U and the outcome Y, except through its effect on X. When such a valid instrument exists, projecting both X and Y onto the space spanned by Z and regressing the projected outcome on the projected exposure yields a consistent estimate of the causal effect. In our spatial basis framework, the basis functions $\{h_j\}_{j=1}^d$ can be thought of as candidate instruments. Under Assumption 1, those h_j with $j \in O_X$ act as valid instruments, in the sense that they influence X but not

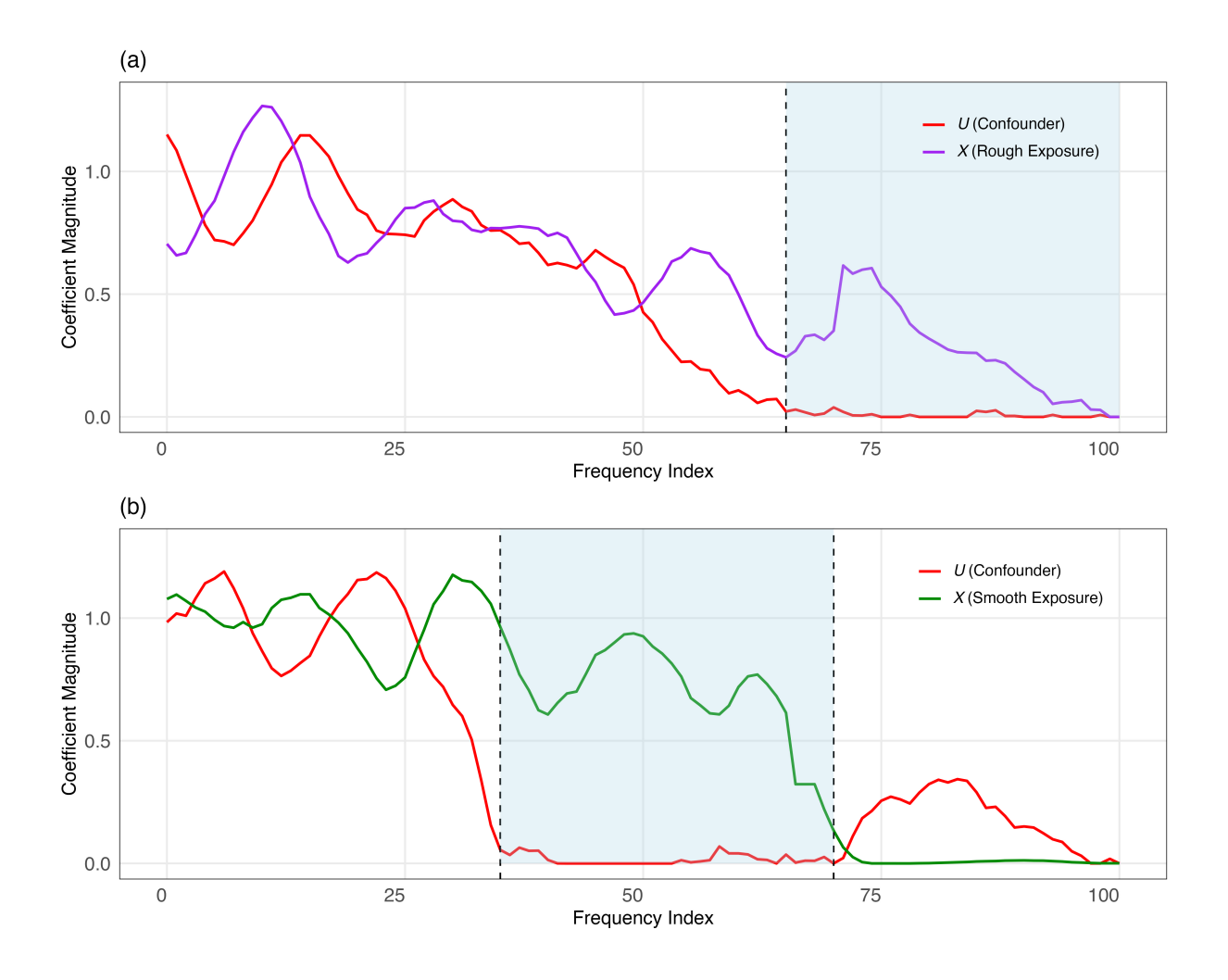


Figure 2: Fourier coefficients of exposures and confounders under varying confounding structures. (a) Exposure X overlaps with unmeasured confounder U at low frequencies, but their behavior diverges at higher frequencies, where U fades and X retains support. (b) X shares low-frequency components with U but decays faster, indicating a smoother exposure than U with an unconfounded region in the middle frequencies. In both Figures, shaded regions mark unconfounded frequency ranges.

U, and hence satisfy the classical exclusion restriction. The remaining basis functions h_j for $j \notin O_X$ are *invalid instruments*, since they affect both X and U, and their use would introduce bias into causal effect estimation.

To illustrate this connection, suppose we knew the set O_X . Then, we could project X and

Y onto the span of $\{h_j : j \in O_X\}$ denoting these projections as $P_{O_X}X$ and $P_{O_X}Y$ and fit a simple linear regression:

$$\hat{\beta} = \frac{\langle P_{O_X} X, P_{O_X} Y \rangle_2}{\langle P_{O_X} X, P_{O_X} X \rangle_2}$$

which yields a consistent estimator of the true effect β . This procedure is directly analogous to two-stage least squares (2SLS), where the projections correspond to first-stage instrumented values. This IV-based perspective is consistent with the framework of Woodward et al. (2024), who show how a variety of existing approaches to unmeasured spatial confounding can be unified under a common IV interpretation.

The challenge, of course, is that O_X is unknown as we no longer assume that the unconfounded variation in X is at the end of the frequency spectrum. Since we do not observe U, we cannot directly verify which basis functions satisfy the exclusion restriction. In the classical IV literature, several recent approaches have been developed to address this problem using methods such as Lasso-based IV selection, robust IV estimators, and plurality-rule estimators (e.g., Kang et al. (2016), Windmeijer et al. (2019)). In particular, plurality-based estimators operate under the assumption that the largest subset of candidate instruments satisfying a particular identifying condition (e.g., validity or consistency of $\hat{\beta}$) corresponds to the correct causal signal. A similar idea has been explored in the time-series setting with unmeasured temporal confounders by Schur & Peters (2024), who project both X and U onto a collection of basis functions and define aggregate estimators from these projections based on a majority-type rule (proportion of invalid candidates is less than 50%), which is a special case of the plurality rule. They frame this problem as an adversarial outlier problem and use robust regression techniques to estimate the effect size, based on a userspecified upper bound of the set of invalid candidates, which is assumed to be decreasing with sample size.

Inspired by these ideas, we propose a plurality-rule estimator which is defined as the mode

of a set of candidate estimators where each candidate is constructed based on each of the spatial basis functions $\{h_j\}_{j=1}^d$. This approach allows us to recover β even without knowledge of O_X , under a plurality assumption that enough of the candidate basis functions are valid (i.e., contribute to X but not U). In the next section, we formally define the plurality-rule assumption and our estimator, present its theoretical guarantees, and describe its advantages in comparison to existing approaches.

3 Plurality Rule Mode Estimator

In analogy to instrumental variables, a basis function h_j is appropriate for constructing a candidate estimator $\hat{\beta}_j$ if it captures variation in the exposure but not in the unmeasured confounder. Such a direction isolates unconfounded exposure variation, enabling consistent estimation of the exposure's effect on the outcome. In the basis representation of the exposure X and the unmeasured confounder U in Section 2, projections of a basis function h_j on them are given by the coefficients $\alpha_x^{(j)}$ and $\alpha_u^{(j)}$. Thus a basis function h_j is an ingredient of a valid candidate if $j \in O_X$, i.e., $\alpha_u^{(j)}/\alpha_x^{(j)} = 0$. On the other hand h_j (and, $\hat{\beta}_j$) will be invalid if $\alpha_u^{(j)}/\alpha_x^{(j)} = \nu$ for some invalidity level $\nu \neq 0$. Causal methods handle multiple IVs of unknown validity based on assumptions about the number of valid instruments. The majority rule assumes that more than 50% of the candidate instruments are valid, in which case β can be identified by simply using the median of the candidate instrument-based estimators. In the context of spatial confounding, saying that the confounder is not supported by over half the basis set is a strong assumption.

Plurality rule clusters the basis functions h_j in terms of the ratio ν , and posits that the biggest cluster is at 0. Of course, if majority rule holds then the cluster at 0 includes more than 50% of the basis, and plurality rule automatically holds. Hence, plurality is a weaker assumption than majority. In fact, plurality does not enforce any minimal cardinality of

 O_X , which can be as low as 2 (if the remaining ratios are all unique) as instead of the median we will use a mode based estimator. We define the plurality rule formally below. Note that we will denote in-probability convergence using $\frac{P}{n\to\infty}$ and weak convergence using $\frac{d}{n\to\infty}$ throughout.

We define the set $S_{x,d} = \{1 \le k \le d : \alpha_x^{(k)} \ne 0\}$, that is, the set denoting the indices of the basis functions which have non-zero projection on X. This set is identifiable because we observe X and we can find the projection $\alpha_x^{(k)}$ of X on each h_k filtering it based on a suitable small threshold to determine which k lies in $S_{x,d}$. Next, we define the set of confounder-exposure projection ratios for the basis functions with indices in the set $S_{x,d}$ as:

$$R_d = \left\{ r_{k,d} := \frac{\alpha_u^{(k)}}{\alpha_x^{(k)}} : k \in S_{x,d} \text{ i.e } \alpha_x^{(k)} \neq 0 \right\}$$
 (2)

Let $C_n = \{\hat{\beta}_{k,n} : k \in S_{x,d}\}$ be a class of candidate estimators, where $\hat{\beta}_{k,n}$ corresponds to the basis function h_k such that for each $k \in S_{x,d}$, $\hat{\beta}_{k,n} \xrightarrow{P} \beta + r_{k,d}$. Specific candidate estimators will be presented in Section 4, but the main idea of the plurality-rule based estimator that we discuss in this section is agnostic to this choice. For any $\nu \in \mathbb{R}$, define

$$\mathcal{I}_{\nu} = \{ r_{k,d} \in R_d : r_{k,d} = \nu \} \tag{3}$$

Then, $k \in O_X \iff r_{k,d} \in \mathcal{I}_0$ and this one-to-one correspondence gives us the rationale for the next assumption, which will help us estimate β without the knowledge of O_X : **Assumption 2** (Plurality Assumption). $|\mathcal{I}_0| > \max_{\nu \neq 0} |\mathcal{I}_{\nu}|$.

Under this assumption, the cluster of ratios $r_{k,d}$ at 0 is larger than clusters at any other real number ν , implying that the mode of the set R_d is 0. To illustrate this is a reasonable assumption in real world applications, we chose the TerraClimate dataset (Abatzoglou et al. (2018)), which provides monthly climate variables globally at ~ 4 km spatial resolution. Specifically, we extracted two meteorological variables, namely monthly minimum temperature (°C) and total precipitation (mm), for the year 2024, averaged them over the 12

months, and restricted the domain to the contiguous United States. These variables have an empirical correlation of 0.42, and in an analysis either of them can play the role of an exposure or an unmeasured confounder. Here, we have considered a set of basis functions that are the cartesian product of two one-dimensional Fourier basis functions and thus lack the natural roughness ordering among them. These annual mean fields were then projected onto this basis function set and we looked at both the basis coefficients as well as the mode of R_d for varying choices of d. Figure 3 presents the illustration.

We see from comparing Panels (a) and (b) that the map of temperature looks much smoother than that of precipitation. This is also confirmed by the basis coefficient plots in panels (c.1) and (c.2) showing that the support of precipitation has a much longer tail. Existing spatial deconfounding methods would thus do well when the precipitation is the exposure and the temperature is the unmeasured confounder but not the other way around. To assess whether the plurality rule holds in either direction, we plot the modes of R_d as a function of d both ways – with precipitation as confounder and temperature as exposure in Panel (d), and vice versa in Panel (e). We see that in both plots, the modes decay to 0 as d increases, suggesting that the plurality rule is satisfied in either direction, and estimators based on the plurality rule can account for a wider range of scenarios of spatial confounding.

We formalize the estimation below. As $\hat{\beta}_{k,n} \xrightarrow{P} \beta + r_{k,d}$, if the mode of R_d is 0, intuitively the mode of C_n will be $\beta + \text{mode}(R_d) = \beta$. Thus the mode of the candidate estimators can be a good estimator for β . In practice, as C_n is a finite set, it is likely that each value of $\hat{\beta}_{k,n}$ will be unique. So we will use a kernel density smoothing to estimate the mode.

Definition 1. For a symmetric Kernel function K, and a finite set $\mathbf{a}_m = \{a_1, \dots, a_m\}$ with each $a_i \in \mathbb{R}$, we can define a Kernel Density, with bandwidth h, as:

$$KD(\boldsymbol{a}_m, K, h, x) = \frac{1}{mh} \sum_{i=1}^m K\left(\frac{x - a_i}{h}\right).$$

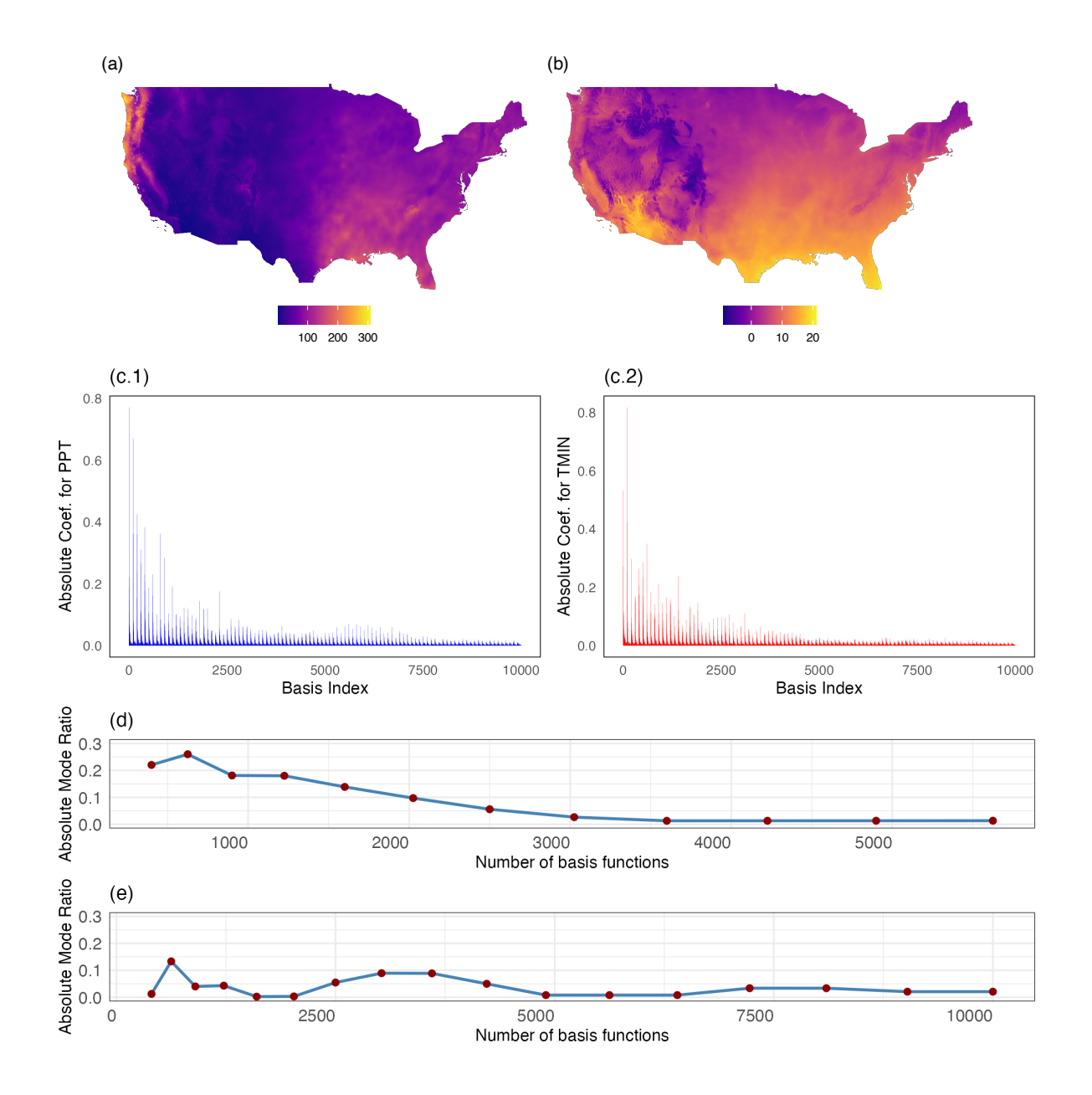


Figure 3: (a) Annual mean precipitation (Ppt) in mm and (b) annual mean minimum temperature (Tmin) in °C for 2024 over the contiguous U.S. Absolute Fourier basis coefficients for (c.1) Ppt and (c.2) Tmin using 10,000 basis functions. Absolute density mode of coefficient ratios: (d) Ppt/Tmin and (e) Tmin/Ppt across varying numbers of basis functions.

The following Lemma shows that the mode of a KDE based on a finite set of values with unique mode also has the same mode with a suitably chosen bandwidth.

Lemma 1. If K is Lipschitz continuous and the finite set $a_m = \{a_1, \dots, a_m\}$ has a unique

mode t, then for some h_0 and all $0 < h \le h_0$, where h_0 depends on K and $\min_{a_i \ne t} |t - a_i|$, $\underset{x \in \mathbb{R}}{\operatorname{arg max}} \ KD(\boldsymbol{a}_m, K, h, x) = t$.

Hence, we work with the KDE estimate for a small enough bandwidth which depends on the functional form of the kernel and the separation of 0 from any other mode of the set R_d . As the limit points of C_n are $\{\beta+r_{k,d}:r_{k,d}\in R_d\}$ we then have, $\underset{x\in\mathbb{R}}{\arg\max}\ KD(\beta+R_{k,d},K,h,x)=\beta$ where $\beta+R_d=\{\beta+r_{k,d}:r_{k,d}\in R_d\}$. This motivates us to propose the following ensemble estimator by combining all the candidate estimators from the class C_n :

$$\hat{\beta}_n = mode(\mathcal{C}_n) := \underset{x \in \mathbb{R}}{\operatorname{arg \, max}} \ KD(\mathcal{C}_n, K, h, x). \tag{4}$$

We call our method 'basis voting' as the process to select the final estimator $\hat{\beta}_n$ mimics a voting process. Each basis h_k represents a voter who votes for a candidate $\hat{\beta}_{k,n}$, and the most popular candidate (formally, the KDE mode) among the set of candidates $C_n = \{\hat{\beta}_{k,n}\}$ is the winner (final estimator). The following theorem gives us theoretical guarantees for the mode estimator:

Theorem 1. Consider the class of estimators $C_n = \{\hat{\beta}_{k,n} : k \in S_{x,d}\}$ such that for each $k \in S_{x,d}$, $\hat{\beta}_{k,n} \xrightarrow{P} \beta + r_{k,d}$ where $r_{k,d} \in R_d$ defined in Equation 2, then under Assumption 2, a Lipschitz continuous Kernel K, and bandwidth $h \leq h_0$ as defined in Lemma 1,

$$\hat{\beta}_n = \underset{x \in \mathbb{R}}{\operatorname{arg \, max}} \ KD(\mathcal{C}_n, K, h, x) \xrightarrow[n \to \infty]{P} \underset{x \in \mathbb{R}}{\operatorname{arg \, max}} \ KD(\{\beta + r_{k,d} : r_{k,d} \in R_d\}, K, h, x) = \beta.$$

Hence, we have a consistent estimator of β under the plurality rule without any assumptions on the exposure being rougher than the confounder. As we see, the consistency of the ensemble model estimator relies on consistency of candidate estimators $\hat{\beta}_{k,n}$ to the respective limits $\beta + r_{k,d}$. In order to get good, efficient estimates of β , we need to have our candidate estimators be well-behaved and have efficient rates of convergence towards their limits. The following section presents choices of such candidate estimators.

4 Candidate Estimators

The building blocks of the mode estimator $\hat{\beta}_n$ are the candidate estimators $\hat{\beta}_{j,n}$ and thus we need to have efficient choices for them. In this section, we present two sets of candidates. We start with the classical projection-based estimator commonly used in the causal inference literature, and then we will introduce a new class of candidate estimators, comparing its performance with the former one. Our goal in this section is to demonstrate how our new candidate estimates can improve on both bias and efficiency in estimating the causal effect β . We define some notations that we will be using to define our candidate estimators. For a given set of sampled spatial coordinates (S_1, \ldots, S_n) , let $\mathbf{h}_{n,j} = (h_j(S_1), \ldots, h_j(S_n))^{\top}$ denote the vector of evaluated values for the basis h_j . Also let us denote $\mathbf{H}_{1:k} = \begin{bmatrix} \mathbf{h}_{n,1} & \cdots & \mathbf{h}_{n,k} \end{bmatrix}$ the evaluation matrix for first k basis functions and corresponding projection on its column space as $\mathbf{P}_k = \mathbf{H}_{1:k} \left(\mathbf{H}_{1:k}^{\top} \mathbf{H}_{1:k} \right)^{-1} \mathbf{H}_{1:k}^{\top}$. Define the projected exposures and outcomes on the first d basis as $\mathbf{X}_{n,d} = \mathbf{P}_d \mathbf{X}_n$ and $\mathbf{Y}_{n,d} = \mathbf{P}_d \mathbf{Y}_n$.

4.1 Projection-Based Estimator

We begin with a standard projection-based candidate estimator that aligns closely with classical approaches. In the context of time-series deconfounding, this candidate has been used by (Schur & Peters 2024) under a special case of the plurality-type assumption. Consider any single basis function $h_j(\cdot)$ with index $j \in S_{x,d}$, indicating that h_j contributes to the spatial variation in the exposure X. We use this basis function to define a classic Two-Stage Least Squares (2SLS) estimator. The projection matrix onto $\mathbf{h}_{n,j}$ is given by $\mathbf{P}_{n,j} := \mathbf{h}_{n,j} \left(\mathbf{h}_{n,j}^{\top} \mathbf{h}_{n,j}\right)^{-1} \mathbf{h}_{n,j}^{\top}$. Then, for any $j \in S_{x,d}$, the projection candidate is computed as the OLS between the projections of the outcome and the exposure, i.e.,

$$\hat{\beta}_{j,n}^{PROJ} := \left[(\boldsymbol{P}_{n,j} \boldsymbol{X}_n)^{\top} (\boldsymbol{P}_{n,j} \boldsymbol{X}_n) \right]^{-1} (\boldsymbol{P}_{n,j} \boldsymbol{X}_n)^{\top} \boldsymbol{P}_{n,j} \boldsymbol{Y}_n$$
 (5)

Conditional on the sampled locations $\mathbf{S}_n = (S_1, \dots, S_n)^{\top}$, $\mathbb{E}\left[\hat{\beta}_{j,n}^{PROJ}\right] = \beta + \frac{\mathbf{h}_{n,j}^{\top} \mathbf{U}_n}{\mathbf{h}_{n,j}^{\top} \mathbf{X}_n}$. The following theorem provides large sample properties of the estimator.

Theorem 2. Under the DGP as in Equation 1 and the estimator as in Equation 5, assuming a sampling density $f_S > 0$ on the compact domain \mathcal{D} for the i.i.d. sampled coordinates with $\epsilon(S_i)|S_i$'s being i.i.d with mean 0 and variance σ_{ϵ}^2 , defining $r_{j,d} = \alpha_u^{(j)}/\alpha_x^{(j)}$ such that $j \in S_{x,d}$, we have:

(a)
$$\hat{\beta}_{j,n}^{PROJ} \xrightarrow[n \to \infty]{P} \beta + r_{j,d}$$

$$\begin{array}{l} (b) \ \sqrt{n} \left(\hat{\beta}_{j,n}^{PROJ} - (\beta + r_{j,d}) \right) \xrightarrow[n \to \infty]{d} N \left(0, \sigma_{j,d}^2 \right) \\ where \ \sigma_{j,d}^2 \coloneqq \frac{\sigma_{U,j}^2 + \sigma_{\epsilon}^2}{\alpha_x^{(j)^2}} + \alpha_u^{(j)} \left(\frac{\alpha_u^{(j)}}{\alpha_x^{(j)^4}} \sigma_{X,j}^2 - \frac{2}{\alpha_x^{(j)^3}} \sigma_{U,X,j} \right) for \ \sigma_{U,j}^2 \coloneqq \|h_j U\|_{f_S}^2 - \alpha_u^{(j)^2}, \ \sigma_{X,j}^2 \coloneqq \|h_j X\|_{f_S}^2 - \alpha_x^{(j)^2} \ and \ \sigma_{U,X,j} \coloneqq \langle h_j X, h_j U \rangle_{f_S} - \alpha_u^{(j)} \alpha_x^{(j)}. \end{array}$$

The theorem proves that the projection-based candidate estimators $\hat{\beta}_{j,n} \xrightarrow{P} \beta + r_{j,d}$ thereby satisfying the requirement to be used for the mode estimator (4). It also provides the asymptotic variance of the candidates, which, as we will show, is important in determining efficiency. An immediate corollary from the theorem is the consistency and asymptotic normality of the valid projection candidates.

Corollary 1. Under the setup mentioned in Theorem 2, for any $j \in O_X$ defined in Assumption 1, we have $\hat{\beta}_{j,n}^{PROJ} \xrightarrow[n \to \infty]{P} \beta$, and after proper scaling, we have the asymptotic distribution $\sqrt{n} \left(\hat{\beta}_{j,n}^{PROJ} - \beta \right) \xrightarrow[n \to \infty]{d} N \left(0, \frac{\sigma_{U,j}^2 + \sigma_{\epsilon}^2}{\alpha_x^{(j)}^2} \right)$ where $\sigma_{U,j}^2 = \|h_j U\|_{f_S}^2$.

The corollary can be deduced directly from Theorem 2 by setting $\alpha_u^{(j)} = 0$ as $j \in O_X$. This implies that if we can choose a valid basis function h_j , i.e., h_j is present in the expansion of X and not in the expansion of U, then we can get a consistent estimate of β . Note that, excluding pathological cases, $\sigma_{U,j}^2 = \int_{\mathcal{D}} (h_j(s)U(s))^2 f_S(s)ds - \alpha_u^{(j)^2} = \operatorname{Var}(h_j(S)U(S)) > 0$ even if $\alpha_u^{(j)} = 0$. So the asymptotic variance of $\hat{\beta}_{j,n}^{PROJ}$ is strictly greater than $\sigma_{\epsilon}^2/\alpha_x^{(j)^2}$. This inequality has important consequences on the efficiency of the projection estimator,

as we will show later.

4.2 Drop-One Estimator

As seen in the previous section is that the projection based method estimator, although is consistent for large samples has a finite-sample bias $h_{n,j}^{\top} X_n$. Even when $j \in O_X$, and the term vanishes asymptotically, it still contributes to the asymptotic variance of $\hat{\beta}_{j,n}^{PROJ}$. We present an improved candidate estimator by including basis functions from the set \mathcal{H}_U in Figure 1. These variables support U but not X and are thus not part of the confounding mechanism. They are often termed as "precision variables" in the causal literature, as including them in the regression helps explain more of the outcome variance, thereby increasing precision of the estimator. For $j \in \{1, \dots, d\}$, define the matrix $\mathbf{H}_{-j|1:d} = \begin{bmatrix} \mathbf{h}_{n,1} & \dots & \mathbf{h}_{n,j-1} & \mathbf{h}_{n,j+1} & \dots & \mathbf{h}_{n,d} \end{bmatrix}$ i.e. the first d basis evaluations dropping the j-th one. We can decompose $U(s) = \sum_{l=1}^{\infty} \alpha_u^{(l)} h_l(s) = \alpha_u^{(j)} h_j(s) + \sum_{l\neq j}^{d} \alpha_u^{(l)} h_l(s) + (1-\lambda_d) U_{>d}(s)$ for $1 \leq j \leq d$, where $\lambda_d = 1$ if U has support only on the first d basis functions and 0 otherwise and hence $U_{>d}(s) = \sum_{l=d+1}^{\infty} \alpha_u^{(l)} h_l(s)$. Hence we can write $\mathbf{U}_n = \alpha_u^{(j)} \mathbf{h}_{j,n} + \mathbf{H}_{-j|1:d} \boldsymbol{\alpha}_{-j,u} + (1-\lambda_d) U_{n,>d}$ where $\boldsymbol{\alpha}_{-j,u} = \left(\alpha_u^{(1)}, \dots, \alpha_u^{(j-1)}, \alpha_u^{(j+1)}, \dots, \alpha_u^{(d)}\right)^{\top}$. If $j \in O_X$, this simplifies to $\mathbf{U}_n = \mathbf{H}_{-j|1:d} \boldsymbol{\alpha}_{-j,u} + (1-\lambda_d) U_{n,>d}$. Thus, the DGP for the observed values projected onto the first d basis functions can be written as:

$$\mathbf{Y}_{n,d} = \mathbf{P}_{d}\mathbf{Y}_{n} = \beta \mathbf{P}_{d}\mathbf{X}_{n} + \mathbf{P}_{d}\mathbf{H}_{-j|1:d}\boldsymbol{\alpha}_{-j,u} + \alpha_{u}^{(j)}\mathbf{P}_{d}\mathbf{h}_{j,n} + (1 - \lambda_{d})\mathbf{P}_{d}\mathbf{U}_{n,>d} + \mathbf{P}_{d}\boldsymbol{\epsilon}_{n}$$

$$= \beta \mathbf{X}_{n,d} + \mathbf{H}_{-j|1:d}\boldsymbol{\alpha}_{-j,u} + \alpha_{u}^{(j)}\mathbf{h}_{j,n} + (1 - \lambda_{d})\mathbf{P}_{d}\mathbf{U}_{n,>d} + \mathbf{P}_{d}\boldsymbol{\epsilon}_{n}$$

$$= \left[\mathbf{X}_{n,d} \quad \mathbf{H}_{-j|1:d}\right] \begin{bmatrix} \beta \\ \boldsymbol{\alpha}_{-j,u} \end{bmatrix} + \alpha_{u}^{(j)}\mathbf{h}_{j,n} + (1 - \lambda_{d})\mathbf{P}_{d}\mathbf{U}_{n,>d} + \mathbf{P}_{d}\boldsymbol{\epsilon}_{n}$$

$$\stackrel{\cdot}{=} \tilde{\mathbf{X}}_{-j}\boldsymbol{\gamma}_{-j,u} + \alpha_{u}^{(j)}\mathbf{h}_{j,n} + (1 - \lambda_{d})\mathbf{P}_{d}\mathbf{U}_{n,>d} + \mathbf{P}_{d}\boldsymbol{\epsilon}_{n}$$

$$\stackrel{\cdot}{=} \tilde{\mathbf{X}}_{-j}\boldsymbol{\gamma}_{-j,u} + \alpha_{u}^{(j)}\mathbf{h}_{j,n} + (1 - \lambda_{d})\mathbf{P}_{d}\mathbf{U}_{n,>d} + \mathbf{P}_{d}\boldsymbol{\epsilon}_{n}$$

Thus if $j \in O_X$, the second term above is 0. Also, as the columns of P_d are asymptotically uncorrelated with $U_{n,>d}$, $P_dU_{n,>d}/n$ vanishes asymptotically. Hence, for $j \in O_X$, we can

write the regression as

$$\mathbb{E}\left[\frac{1}{n}Y_{n,d}\right] pprox \frac{1}{n}\tilde{X}_{-j}\gamma_{-j,u},$$

where the first element of $\gamma_{-j,u}$ is β . Hence, the first element of the OLS estimate of $Y_{n,d}$ on \tilde{X}_{-j} is a consistent estimate for β . Equivalently, if we do a two-stage regression, first regressing $Y_{n,d}$ on everything but the first column of \tilde{X}_{-j} , i.e., on $H_{-j|1:d}$, and then regress the residual on the first column of \tilde{X}_{-j} , i.e., $X_{n,d}$, we should have a consistent estimator of β . This motivates the following drop-one estimator

$$\hat{\beta}_{-j,n} = \frac{\boldsymbol{X}_{n,d}^{\top} (\boldsymbol{I}_n - \boldsymbol{P}_{-j,d}) \boldsymbol{Y}_{n,d}}{\boldsymbol{X}_{n,d}^{\top} (\boldsymbol{I}_n - \boldsymbol{P}_{-j,d}) \boldsymbol{X}_{n,d}}, \text{ where } \boldsymbol{P}_{-j,d} = \boldsymbol{H}_{-j|1:d} \left(\boldsymbol{H}_{-j|1:d}^{\top} \boldsymbol{H}_{-j|1:d} \right)^{-1} \boldsymbol{H}_{-j|1:d}^{\top}.$$
(7)

This candidate estimator is similar in spirit to the residual-on-residual regression proposed by Thaden & Kneib (2018), although we only use it as a candidate estimator fed into our ensemble mode estimator of Section 3, thereby allowing us to relax the assumption of rough exposure as considered there. The drop-one candidate estimator incorporates more information about the data into the regression of $Y_{n,d}$ on \tilde{X}_{-j} as compared to the projection method, where we were choosing one basis function at a time, and hence the former should be statistically more efficient. The following theorem shows the performance of the drop-one estimator in large samples:

Theorem 3. Under the DGP as in Equation 1 and the estimator as in Equation 7, assuming a sampling density $f_S > 0$ on the compact domain \mathcal{D} for the i.i.d. sampled coordinates with $\epsilon(S_i)|S_i$'s being iid with mean 0 and variance σ_{ϵ}^2 , defining $r_{j,d} = \alpha_u^{(j)}/\alpha_x^{(j)}$ such that $j \in S_{x,d}$, we have:

(a)
$$\hat{\beta}_{-j,n} \xrightarrow[n \to \infty]{P} \beta + r_{j,d}$$
.

(b) For any
$$j \in O_X$$
, we have $\sqrt{n} \left(\hat{\beta}_{-j,n} - \beta \right) \xrightarrow[n \to \infty]{d} N \left(0, \frac{(1-\lambda_d)\sigma_{U,j,>d}^2 + \sigma_{\epsilon}^2}{\alpha_x^{(j)^2}} \right)$ where $\sigma_{U,j,>d}^2 := Var(h_j U_{>d}) = \|h_j U_{>d}\|_{f_{\mathfrak{C}}}^2$.

(c) If
$$\lambda_d = 1$$
, then for $j \in O_X$ we have $\mathbb{E}\left[\hat{\beta}_{-j,n}\right] = \beta$.

The first two results are similar to those in Theorem 2, establishing consistency and asymptotic normality of the candidate drop-one estimators. Additionally, if U admits a finite basis expansion with respect to \mathcal{H} which is implictly assumed by many existing spatial deconfounding approaches, e.g., the spline-based adjustment of Keller & Szpiro (2020), the third result shows that additionally $\hat{\beta}_{-j,n}$ is exactly finite-sample unbiased for any $j \in O_X$. This unbiasedness property is an improvement over the projection-based estimator which always has a finite-sample bias.

4.3 Comparison of Drop-one and Projection Method

We now look at the comparison of asymptotic variances of the estimators based on valid candidate basis functions which support X but not U, i.e., h_j for $j \in O_X$. We have seen from Theorems 2 and 3 that for any $j \in O_X$, the candidate's estimates are consistent for β and asymptotically normal with mean β . Also, we can see the asymptotic variance of the scaled drop-one estimator is $avar\left(\hat{\beta}_{-j,n}\right) = \frac{(1-\lambda_d)\sigma_{U,j,>d}^2+\sigma_\epsilon^2}{\alpha_x^{(j)^2}}$ and that for the projection estimator is $avar\left(\hat{\beta}_{j,n}^{PROJ}\right) = \frac{\sigma_{U,j}^2+\sigma_\epsilon^2}{\alpha_x^{(j)^2}}$. Once again, under an assumed finite basis representation of U, the term $(1-\lambda_d)\sigma_{U,j,>d}^2$ vanishes and because $\sigma_{U,j}^2>0$ as discussed at the end of section 4.1, we immediately have that:

$$avar\left(\hat{\beta}_{-j,n}\right) < avar\left(\hat{\beta}_{j,n}^{PROJ}\right),$$

i.e., our proposed drop-one candidate is more efficient than the projection candidate.

The following lemma shows that the result holds even if U has infinite expansion for many choices of basis functions.

Lemma 2. Let $\mathcal{H} = \{h_j\}_{j\geq 1}$ be orthonormal in $\mathcal{L}^4(\mathcal{D}, f_S)$, with $U = \sum_{j\geq 1} \alpha_u^{(j)} h_j$, $U_{\leq d} = \sum_{j\leq d} \alpha_u^{(j)} h_j$, $U_{>d} = \sum_{j>d} \alpha_u^{(j)} h_j$ for $d \in \mathbb{N}$ and define $S_{\text{in}} := \sum_{j\leq d} \alpha_u^{(j)^2}$. Assume:

(i)
$$\max_{1 \le j \le d} ||h_j||_{\infty} \le M < \infty$$
.

(ii) For each $j \leq d$, the zero set $\{s : h_j(s) = 0\}$ has f_S -measure 0 (equivalently, $h_j^2 > 0$ f_S -a.e.).

(iii)
$$||U_{>d}||_{f_S}^2 \le \varepsilon$$
 with $\varepsilon < \frac{c_*}{4M^2} S_{\text{in}}$, where for $V_j := \text{span}\{h_k : k \le d, k \ne j\}$,

$$c_* := \min_{1 \le j \le d} \inf_{\substack{v \in V_j \\ \|v\|_{f_S} = 1}} \int_{\mathcal{D}} h_j^2 v^2 f_S ds > 0$$

Then for every j = 1, ..., d with $j \in O_X$ i.e. $\alpha_u^{(j)} = 0$,

$$||h_j U||_{f_S}^2 > ||h_j U_{>d}||_{f_S}^2.$$

Using this lemma, it can be directly inferred from Theorems 2 and 3 that $\sigma_{U,j}^2 > \sigma_{U,j,>d}^2$ for $j \in O_X$. Thus even for U having possibly infinite expansion i.e. for $\lambda_d = 0$, if \mathcal{H} satisfies the assumptions of Lemma 2, then:

$$avar\left(\hat{\beta}_{-j,n}\right) < avar\left(\hat{\beta}_{j,n}^{PROJ}\right).$$

The first two assumptions of Lemma 2 (where $||h_j||_{\infty} := \sup_s |h_j(s)|$) are not restrictive and are satisfied by most of the standard families of basis functions used for analysis in a compact spatial domain, such as Fourier basis and polynomial basis classes. The third assumption is not specific to any basis class and is satisfied for a choice of d that is sufficiently large. The fact that $c^* > 0$ can be derived from Assumption (ii) of the lemma, more details about which can be found in the Appendix. This shows that the drop-one candidate estimator is more efficient than the standard projection-based estimator under a broad range of scenarios, motivating its use in the ensemble mode estimator of Section 3.

5 Simulation Study

5.1 Simulation Data Generation

To investigate the performance of the proposed estimator under controlled conditions, we have conducted a comprehensive simulation study. The primary goal of the simulation was to evaluate whether basis voting could recover the causal effect β in the presence of unmeasured spatial confounding, when the structure of confounding aligns with our identification assumptions, which may or may not match with that of the existing methods. We considered a spatial domain $\mathcal{D} = [0,1]^2$, where the spatial coordinates were chosen as a grid inside it. For the main simulations, we used a regular grid design with $n = 30^2 = 900$

grid inside it. For the main simulations, we used a regular grid design with $n=30^2=900$ spatial locations. At each location, both the exposure X(s) and the unmeasured confounder U(s) were generated as linear combinations of a common set of spatial basis functions, constructed from sine and cosine transforms of spatial coordinates, i.e., the Fourier basis functions. This construction allowed us to control the smoothness and spatial scale of both the exposure and the confounder. The coefficients for X and U on the basis functions were chosen to emulate realistic confounding while ensuring that the ratio $\alpha_u^{(j)}/\alpha_x^{(j)}$ has a well-separated mode at zero. Specifically, the coefficients were designed such that a subset of basis functions contributed to both X and U (i.e., confounded directions) while some basis functions were exclusive to either X or U.

The non-zero values of the exposure coefficients vector $\{\alpha_x^{(j)}\}$ and confounder coefficients vector $\{\alpha_u^{(j)}\}$ were sampled independently from Unif(3,6) distribution along with random sign $\{-1,1\}$ assigned with equal probability. The coefficients were kept fixed over all the data replicates as we are in a deterministic function scenario. The magnitude of the confounding bias in naive OLS was calibrated based on the inner product of the coefficient vectors, ensuring a challenging identification task.

The observed outcome was generated using the structural equation $Y(s) = \beta X(s) + U(s) + \epsilon(s)$ where $\beta = 2.5$ is the true causal effect, and $\epsilon(s) \sim \mathcal{N}(0, \sigma_{\epsilon}^2)$ with $\sigma_{\epsilon} = 0.1$ is i.i.d. noise. Based on whether X is smoother than U or not, there are 2 different DGP scenarios that we have considered.

5.2 Correct Basis Specification

We simulate two distinct scenarios for the exposure X(s) and the unmeasured confounder U(s) to evaluate the performance of our proposed method relative to existing approaches. Specifically, we consider cases where (a) the exposure is a rougher function of space than the confounder, and (b) the exposure is smoother. Many existing methods assume the exposure is spatially rougher than the confounder, and we aim to assess the robustness of our method when this assumption is violated.

Figure 4 compares our proposed estimator to several existing methods, using the oracle estimator as a benchmark (which leverages knowledge of the true shared basis functions for optimal efficiency). Competing methods include Ordinary Least Squares (OLS), Generalized Least Squares (GLS) with a pre-specified exponential covariance kernel using the BRISC R-package (Saha & Datta 2018), the spatial basis adjustment approach using TPRS basis set in a similar essence to Keller & Szpiro (2020) by adding a spline term in the regression (to adjust for the unmeasured confounder U) additional to the exposure of interest, the gSEM method of Thaden & Kneib (2018), the Spatial+ approach of Dupont et al. (2022), and the spectral domain adjustment of Guan et al. (2023). The results reveal important differences in method performance. When the exposure is rougher than the unmeasured confounder with respect to the Fourier basis (Panel (a)), nearly all methods, including ours, accurately recover the true value of $\beta = 2.5$. Only exception is the unadjusted OLS estimator which of course is expected to be biased under confounding. When the expo-

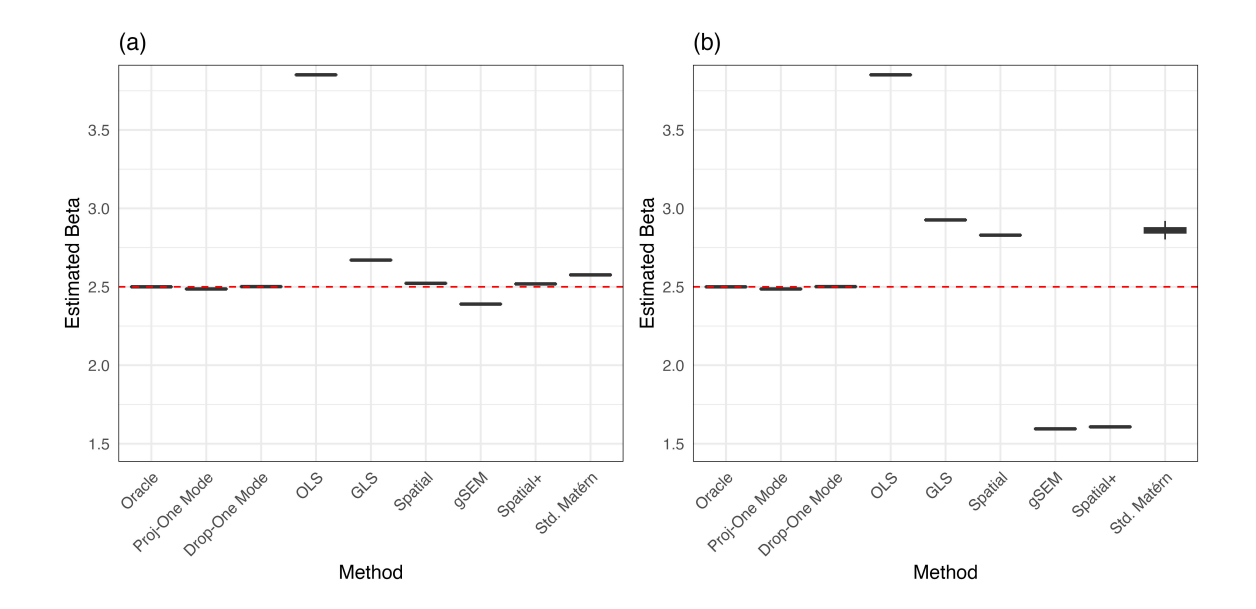


Figure 4: Performance of different methods for estimating $\beta=2.5$ under two scenarios: (a) when the exposure X is rougher than the unmeasured confounder U and (b) when X is smoother than U, using correct basis specification. Our mode-based estimators (named Proj- $One\ Mode$ and Drop- $One\ Mode$) recover the effect sizes in both cases; competitors bias when X is smoother.

sure is smoother than the confounder (Panel (b)), all existing methods yield substantially biased estimates, while our mode-based estimators — both project-on-one and drop-one approaches – remain unbiased and accurately estimate β . This experiment highlights the robustness of our method to violation of the rough exposure assumption.

5.3 Robustness to Basis Misspecification

The experiments in the previous section were in the idealized scenario in which the basis functions used for estimation match those that generated the data. Note that using the correct basis is not a requirement for our method, which only requires that the plurality holds under whichever basis set is used in the analysis to represent the exposure and the confounder. Here, we assess the robustness of our method to basis misspecification.

To explore the effect of basis choice, we consider two misspecified alternatives for analyzing the data: (a) standard thin plate regression splines (TPRS), orthogonalised over the set of locations, and (b) eigen functions derived from the empirical covariance structure of the coordinates, where the latter are obtained by eigen decomposition of a Matérn covariance kernel with fixed parameters.

Figure 5 displays the ratios of the projected coefficients for the confounder and exposure, $\alpha_u^{(j)}/\alpha_x^{(j)}$, onto the j-th misspecified TPRS basis function, under two smoothness regimes for X and U. As we see, in both scenarios, the coefficient ratios have the biggest clustering

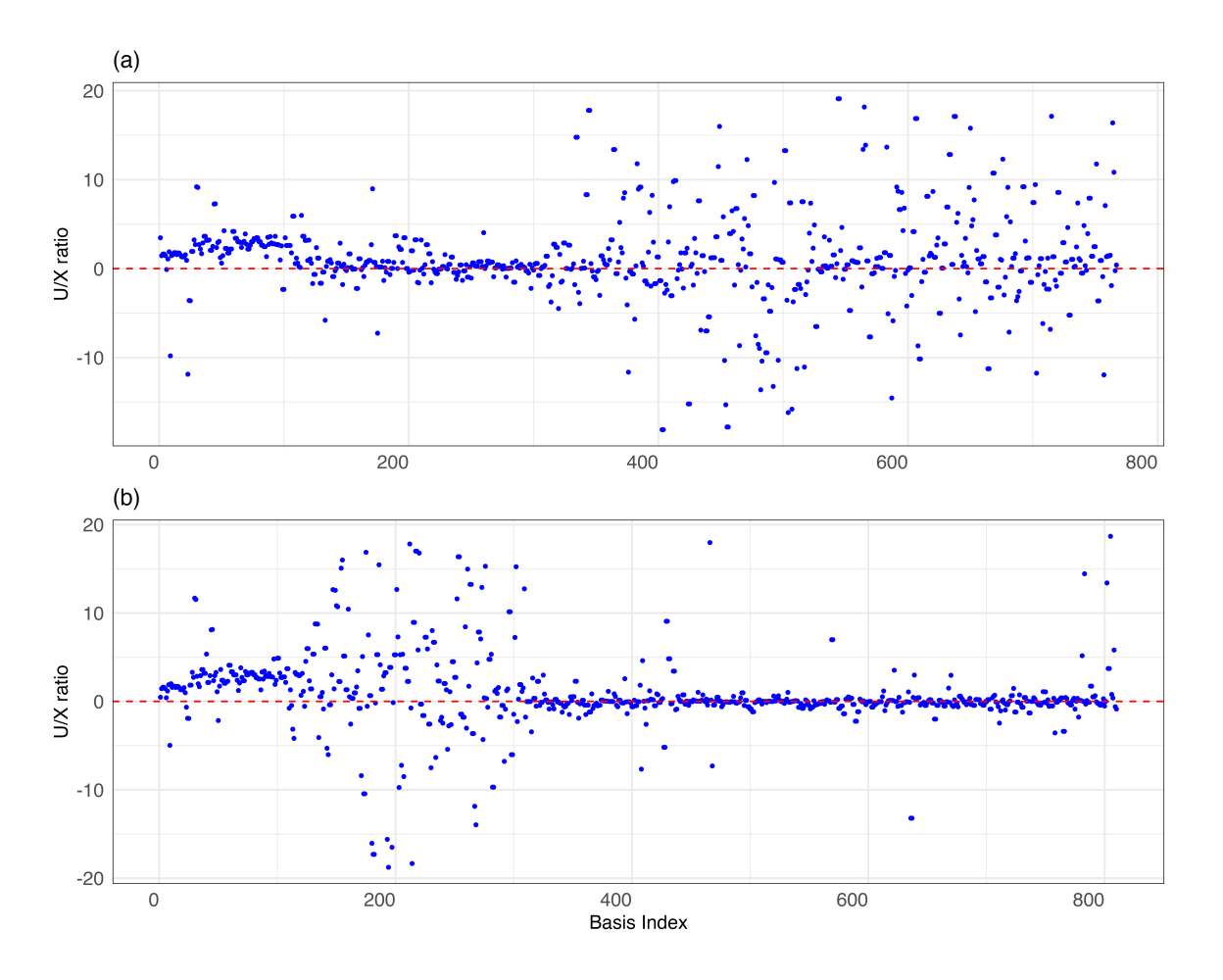


Figure 5: Estimated ratio $\alpha_u^{(j)}/\alpha_x^{(j)}$ for a misspecified TPRS basis under two smoothness scenarios: (a) X is smoother than U, and (b) X is rougher than U.

around the y=0 line, indicating that the modal value remains close to zero. This sup-

ports the validity of Assumption 2 for this class of basis functions, regardless of whether the exposure is smoother or rougher. Similar findings were obtained for the eigen basis functions.

Figure 6 presents the estimated effect sizes produced by our method when using the first d basis functions (with d varying from 150 to 850, for a sample size of 900 observations). Results are presented for both TPRS and eigen basis sets, and under both relative smoothness scenarios for X and U.

These results show that even under basis misspecification, stable estimation of the effect size is attained once a sufficient number of basis functions are included in the model for the plurality rule to kick in. In terms of bias, the projection method performs slightly worse as compared to the drop-one methods in finite samples. Also the projection method exhibits a greater standard error, consistent with the theoretical findings in Section 4.3. We can see that as we go on increasing the number of basis functions in the model, the standard error of the estimates also increases, which is meaningful as we are using more and more variables in the model, which should yield in higher standard error of the estimates, which shows that there is a bias-variance tradeoff here. A higher number of basis functions in the model can definitely help reduce the bias of the estimate, but at the cost of increasing the standard error. Overall, the drop-one candidates based mode estimator is much more robust to the number of basis functions used. The experiments in this section show that our mode estimator works well even with a misspecified basis, both when the exposure is rougher or smoother, and that using the drop-one candidate estimators generally leads to better performance than the projection-based candidate estimators.

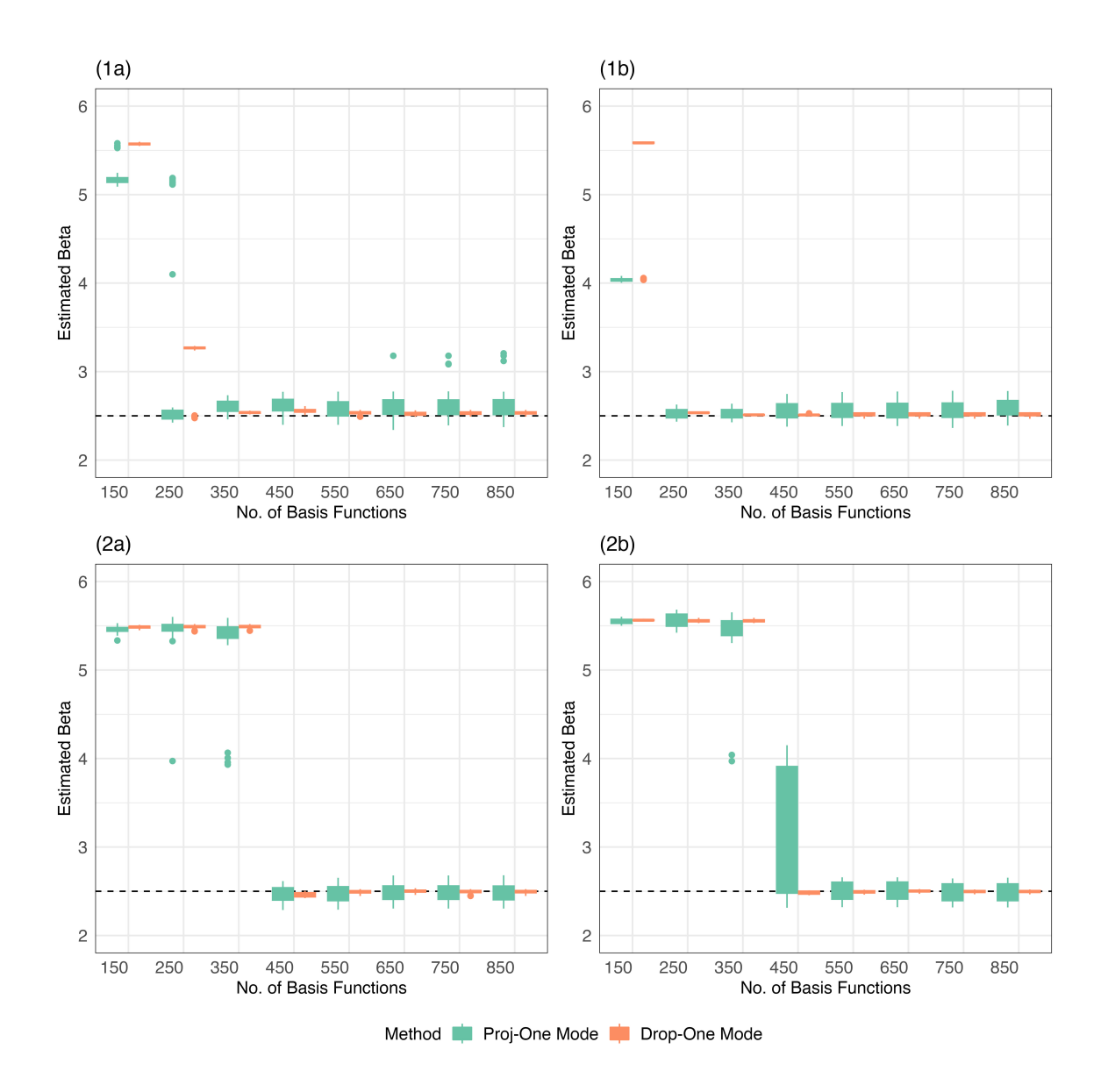


Figure 6: Performance of the two proposed methods under two smoothness scenarios: (1) X is smoother than U, and (2) X is rougher than U, each evaluated with two misspecified basis function types: (a) TPRS basis and (b) Eigen basis functions. The black dotted line is the true effect size $\beta = 2.5$.

6 Real Data Analysis

We illustrate the robustness of our mode estimator in an analysis studying the effect of air quality on COVID-19 mortality. We utilize the county-level COVID-19 dataset analyzed in Guan et al. (2023) and originally collected by Wu et al. (2020), which includes comprehensive information for n=3109 U.S. counties. For each county, the outcome is the cumulative number of COVID-19 deaths through May 12, 2020 (originally obtained from Johns Hopkins University Coronavirus Resource Center), scaled by the county's population. The primary exposure variable is the long-term average $PM_{2.5}$ concentration, computed by averaging estimates from an established exposure prediction model over the years 2000–2016. Figure 7 displays the scaled death counts and $PM_{2.5}$ concentrations for each county. Counties with zero death counts are shown in grey in the figure.

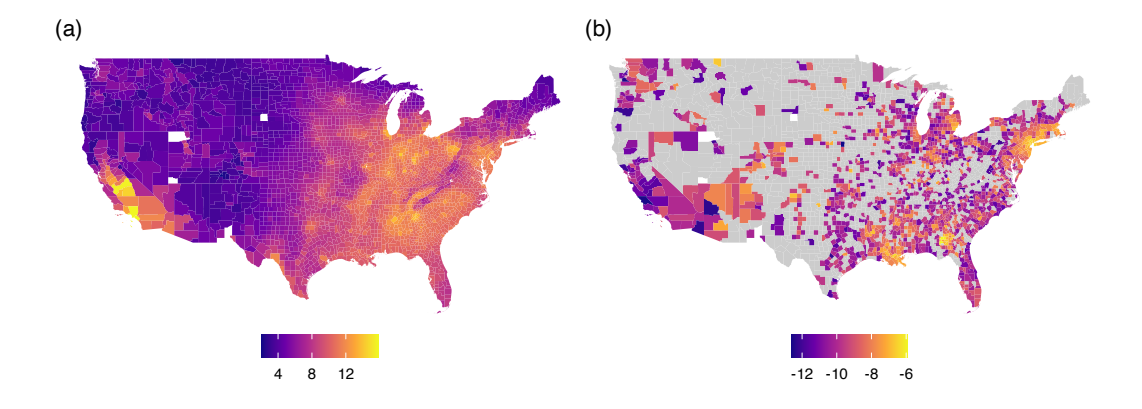


Figure 7: Maps showing (a) Average $PM_{2.5}$ in $(\mu g/m^3)$ for the time period 2000-2016, and (b) the cumulative log COVID-19 mortality rate through May 12, 2020, scaled by population.

In addition to the main exposure and outcome variables, the data set contains 20 additional county-level covariates which are potential confounders. To transform this data into a standard geostatistical one, we assign each county the coordinates of its geographic centroid. Counties for which the boundary centroids could not be calculated were dropped from the

analysis resulting in an effective sample size of n=3082. Consistent with our focus on linear models, we apply a logarithmic transformation to the scaled mortality outcome, replacing zeros with a small positive value to avoid loss of observations and ensure stability of the log transformation. The ordinary least square estimate of the mortality rate ratio for 1 unit increase in $PM_{2.5}$ even after adjusting for the measured confounders is $\exp(-1.286) = 0.267$ which shows a counterintuitive result that higher pollutant levels are protective against COVID-19 mortality. This paradoxical finding is also discussed in Wu et al. (2020) and Guan et al. (2023), and we agree with their conclusion that there is a possibility for the presence of unmeasured spatial confounding.

According to Guan et al. (2023), after adjusting for spatial confounding, the estimated percentage increase in mortality rate associated with a one-unit increase in $PM_{2.5}$ is approximately 16%, i.e., the effect size is around 1.16. To assess the robustness of our proposed approach relative to existing methods that assume an ordered set of basis functions for adjustment, we consider two classes of spatial basis functions: (1) the conventional thin-plate regression splines (TPRS) orthogonalised over the set of locations which exhibit an inherent ordering of smoothness, and (2) the cartesian product of two one-dimensional Fourier bases, which lack such canonical ordering. As a benchmark, we compare our mode-based estimator to the standard basis adjustment approach in regression, which is known to yield consistent results when basis functions are ordered by increasing roughness.

For our analysis, we first regress out the additional covariates from both the exposure and the outcome to enable direct application of our method. Figure 8 compares our estimator to the standard basis adjustment, with the left panel corresponding to the TPRS basis and the right panel to the cartesian product of Fourier basis.

As anticipated, when the basis set has an ordering of smoothness (as with TPRS), the results of both estimators are highly similar and align with the estimate from the previous

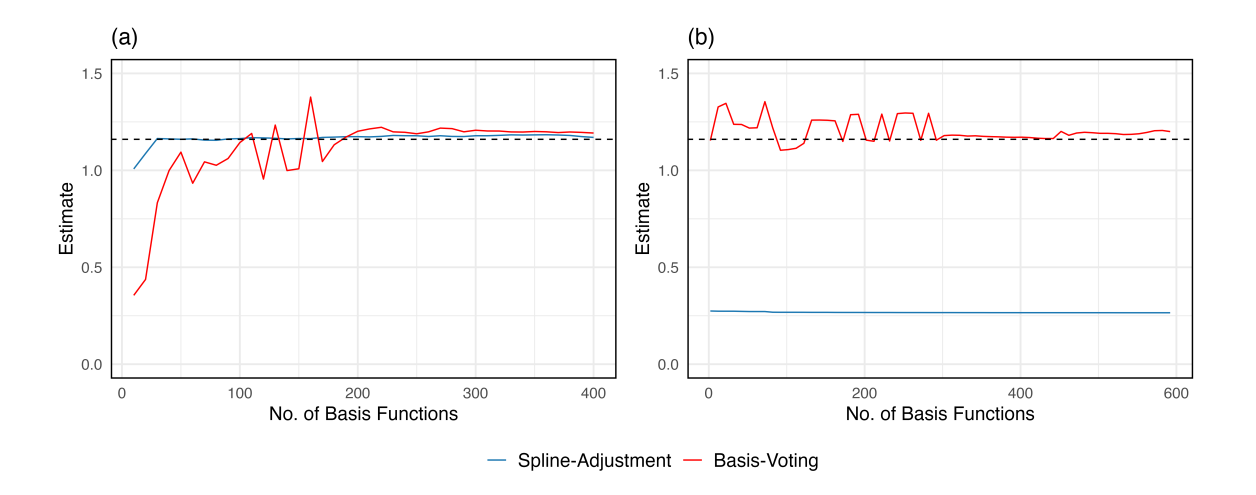


Figure 8: Results for the COVID-19 Data: Estimated mortality-rate ratio for an increase of $1\mu g/m^3$ increase in PM_{2.5} for different numbers of basis functions. The results are for two sets of basis functions: (a) when the basis functions have a canonical ordering of increasing roughness, and (b) when the basis functions do not have a canonical ordering among the basis functions. The blue line is for the model adjusted for k basis functions along with the measured covariates, and the red is for basis voting, our mode-based estimator. Black dotted line is the estimate of 1.16 or 16% reported by Guan et al. (2023).

analyses. Notably, when utilizing the unordered Fourier basis, our mode-based estimator continues to produce estimates close to the presumed effect, whereas the standard basis adjustment method fails to control for unmeasured spatial confounding, producing a very different estimate. This result underscores the advantage of our approach in settings where the exposure does not represent a 'rougher' function of space than the confounder in terms of a given basis expansion.

7 Conclusion and Discussion

Unmeasured spatial confounding poses a major challenge for effect size estimation in spatial linear models, particularly when exposures and confounders share smooth spatial structure.

Existing approaches often assume exposures vary more *roughly* than confounders, but this assumption breaks down in many environmental health settings where exposures themselves are smooth or when using basis functions where there is no single notion of smoothness.

We address this gap by modeling exposures and confounders through basis expansions and emphasizing the fact that a sufficiently large collection of basis functions contributing to the differential support of the exposure is sufficient for identifying the causal effect. Some of the basis functions act as valid candidates, while others induce confounding. Leveraging this structure, we introduce basis voting, a plurality-rule based process to arrive at an estimator that identifies causal effects without requiring prior knowledge of valid bases or bounds on invalid ones. We provide theoretical guarantees for consistency and propose a provably more efficient candidate estimator with improved asymptotic variance. Simulations and a real data analysis confirm that our method delivers unbiased estimates whenever exposure and confounder signals are separable on a plurality of basis functions, regardless of their relative smoothnesses.

This work advances spatial causal inference by relaxing restrictive smoothness assumptions and unifying existing plurality-based strategies under a robust IV perspective. While our framework is limited to linear effects, we plan to explore future extensions to nonlinear models. Also, developing valid statistical inferential procedures using the mode-estimator is an important future direction. Overall, plurality-based estimation provides a flexible and robust tool for addressing spatial confounding in complex applied settings.

8 Acknowledgement

The work was partly supported by National Institute of Health Sciences grant R01 ES033739 and ONR grant N000142412701. The authors acknowledge the use of Chat-GPT.com for improving the exposition in some parts and for some assistance with

developing the theoretical results.

References

- Abatzoglou, J. T., Dobrowski, S. Z., Parks, S. A. & Hegewisch, K. C. (2018), 'Terraclimate, a high-resolution global dataset of monthly climate and climatic water balance from 1958–2015', Scientific data 5(1), 1–12.
- Bolin, D. & Wallin, J. (2024), 'Spatial confounding under infill asymptotics', $arXiv\ preprint$ arXiv:2403.18961.
- Brugge, D., Lane, K., Padró-Martínez, L. T., Stewart, A., Hoesterey, K., Weiss, D., Wang,
 D. D., Levy, J. I., Patton, A. P., Zamore, W. et al. (2013), 'Highway proximity associated with cardiovascular disease risk: the influence of individual-level confounders and exposure misclassification', Environmental health 12, 1–12.
- Casey, J. A., Savitz, D. A., Rasmussen, S. G., Ogburn, E. L., Pollak, J., Mercer, D. G. & Schwartz, B. S. (2016), 'Unconventional natural gas development and birth outcomes in pennsylvania, usa', *Epidemiology* **27**(2), 163–172.
- Clayton, D. G., Bernardinelli, L. & Montomoli, C. (1993), 'Spatial correlation in ecological analysis', *International journal of epidemiology* **22**(6), 1193–1202.
- Currie, J., Greenstone, M. & Meckel, K. (2017), 'Hydraulic fracturing and infant health:

 New evidence from pennsylvania', *Science advances* **3**(12), e1603021.
- Datta, A. & Stein, M. L. (2025), 'Consistent infill estimability of the regression slope between gaussian random fields under spatial confounding', $arXiv\ preprint$ arXiv:2506.09267.

- Dupont, E., Wood, S. N. & Augustin, N. H. (2022), 'Spatial+: a novel approach to spatial confounding', *Biometrics* **78**(4), 1279–1290.
- Gilbert, B., Datta, A., Casey, J. A. & Ogburn, E. L. (2021), 'A causal inference framework for spatial confounding', arXiv preprint arXiv:2112.14946.
- Gilbert, B., Ogburn, E. L. & Datta, A. (2025), 'Consistency of common spatial estimators under spatial confounding', *Biometrika* **112**(2), asae070.
- Guan, Y., Page, G. L., Reich, B. J., Ventrucci, M. & Yang, S. (2023), 'Spectral adjustment for spatial confounding', *Biometrika* **110**(3), 699–719.
- Hodges, J. S. & Reich, B. J. (2010), 'Adding spatially-correlated errors can mess up the fixed effect you love', *The American Statistician* **64**(4), 325–334.
- Kang, H., Zhang, A., Cai, T. T. & Small, D. S. (2016), 'Instrumental variables estimation with some invalid instruments and its application to mendelian randomization', *Journal of the American statistical Association* **111**(513), 132–144.
- Karner, A. A., Eisinger, D. S. & Niemeier, D. A. (2010), 'Near-roadway air quality: synthesizing the findings from real-world data', *Environmental science & technology* **44**(14), 5334–5344.
- Keller, J. P. & Szpiro, A. A. (2020), 'Selecting a scale for spatial confounding adjustment', Journal of the Royal Statistical Society Series A: Statistics in Society 183(3), 1121–1143.
- Khan, K. & Berrett, C. (2023), 'Re-thinking spatial confounding in spatial linear mixed models', arXiv preprint arXiv:2301.05743.
- Khan, K. & Calder, C. A. (2022), 'Restricted spatial regression methods: Implications for inference', *Journal of the American Statistical Association* **117**(537), 482–494.

- Paciorek, C. J. (2010), 'The importance of scale for spatial-confounding bias and precision of spatial regression estimators', *Statistical science: a review journal of the Institute of Mathematical Statistics* **25**(1), 107.
- Page, G. L., Liu, Y., He, Z. & Sun, D. (2017), 'Estimation and prediction in the presence of spatial confounding for spatial linear models', *Scandinavian Journal of Statistics* 44(3), 780–797.
- Reich, B. J., Hodges, J. S. & Zadnik, V. (2006), 'Effects of residual smoothing on the posterior of the fixed effects in disease-mapping models', *Biometrics* **62**(4), 1197–1206.
- Saha, A. & Datta, A. (2018), 'Brisc: bootstrap for rapid inference on spatial covariances', Stat 7(1), e184.
- Schnell, P. M. & Papadogeorgou, G. (2020), 'Mitigating unobserved spatial confounding when estimating the effect of supermarket access on cardiovascular disease deaths', *Annals of Applied Statistics* **14**(4), 2069–2095.
- Schur, F. & Peters, J. (2024), 'Decor: Deconfounding time series with robust regression', arXiv preprint arXiv:2406.07005.
- Thaden, H. & Kneib, T. (2018), 'Structural equation models for dealing with spatial confounding', *The American Statistician* **72**(3), 239–252.
- Vaart, A. v. d. & Wellner, J. A. (1997), 'Weak convergence and empirical processes with applications to statistics', *Journal of the Royal Statistical Society-Series A Statistics in Society* **160**(3), 596–608.
- Wakefield, J. (2007), 'Disease mapping and spatial regression with count data', *Biostatistics* **8**(2), 158–183.
- Windmeijer, F., Farbmacher, H., Davies, N. & Davey Smith, G. (2019), 'On the use of

- the lasso for instrumental variables estimation with some invalid instruments', *Journal* of the American Statistical Association 114(527), 1339–1350.
- Woodard, R., Sun, D., He, Z. & Sheriff, S. L. (1999), 'Estimating hunting success rates via bayesian generalized linear models', *Journal of agricultural, biological, and environmental statistics* pp. 456–472.
- Woodward, S. M., Tec, M. & Dominici, F. (2024), 'An instrumental variables framework to unite spatial confounding methods', arXiv preprint arXiv:2411.10381.
- Wu, X., Nethery, R. C., Sabath, M. B., Braun, D. & Dominici, F. (2020), 'Air pollution and covid-19 mortality in the united states: Strengths and limitations of an ecological regression analysis', *Science advances* **6**(45), eabd4049.
- Zimmerman, D. L. & Ver Hoef, J. M. (2022), 'On deconfounding spatial confounding in linear models', *The American Statistician* **76**(2), 159–167.

SUPPLEMENTARY MATERIAL

S1 Proofs

S1.1 Notations

We denote \mathbb{R} and \mathbb{N} to be the set of real numbers and natural numbers respectively. For a sequence of random variables, $\frac{P}{n\to\infty}$ denotes convergence in probability and $\frac{d}{n\to\infty}$ denotes weak convergence. We will also use stochastic ordering notations throughout the proof. For a sequence of random variable $\{X_n\}$ and a sequence of real numbers $\{a_n\}$, we say $X_n = \mathcal{O}_P(a_n)$ if for all $\epsilon > 0$ there exists a M > 0, such that for all $n \in \mathbb{N}$, we have $\mathbb{P}\left(\left|\frac{X_n}{a_n}\right| > M\right) < \epsilon$. Also, we say $X_n = o_P(a_n)$ if for all $\epsilon > 0$, $\mathbb{P}\left(\left|\frac{X_n}{a_n}\right| > \epsilon\right) \xrightarrow{n\to\infty} 0$. For a real valued function f defined on an inner-product space $(\mathcal{M}, \langle \cdot, \cdot \rangle)$, we denote $\|f(\cdot)\|_{\mathcal{M}} := \sup_{t \in \mathcal{M}} \langle f(t), f(t) \rangle$. All the integrals are over the support \mathcal{D} of the sampling density f_S , and hence unless specified, by f we will mean $f_{\mathcal{D}}$.

S1.2 Proof of Lemma 1

Proof. Recall we denoted the set $\mathbf{a}_m = \{a_1, \dots, a_m\}$ where $m \in \mathbb{N}$ and each of $a_i \in \mathbb{R}$. By the assumption of the lemma, the elements of \mathbf{a}_m have a unique mode at t. Formally, if we define n_a to be the count of the elements of \mathbf{a}_m equaling the value a, then the unique mode assumption can be boiled down to $n_t > \max_{s \in \mathbf{a}_m, s \neq t} n_s$. Let $\delta \coloneqq \min_{s \in \mathbf{a}_m \setminus \{t\}} |t - s| > 0$ and $M \coloneqq \max_{s \in \mathbf{a}_m \setminus \{t\}} n_s$. Let us define the multiplicity gap $\gamma \coloneqq n_t - M > 0$. We consider the two assumptions on K separately.

Case (i) [K has compact support]: Suppose supp $(K) \subseteq [-R, R]$ for some $R < \infty$. Choose $h_0 \in (0, \delta/(2R))$. Then for any $0 < h \le h_0$, each summand $K((x - a_i)/h)$ is supported on an interval of radius $Rh \leq \delta/2$. Hence the n_s bumps centered at a location $s \in \boldsymbol{a}_m$ do not overlap with those centered at any $s' \neq s$. In particular, for $s \in S$, $KD(\boldsymbol{a}_m, K, h, s) = \frac{n_s K(0)}{mh}$, since only the n_s bumps centered at s contribute at s = s, each attaining its maximum s = s, and for some $s' \neq s$, we have $|s - s'|/h > \delta/h > 2R$ which throws the value outside the support of s = s, and we know for s = s outside the support of all bumps, s = s. Therefore,

$$\max_{x \in \mathbb{R}} KD(\boldsymbol{a}_m, K, h, x) = \max_{s \in \boldsymbol{a}_m} KD(\boldsymbol{a}_m, K, h, s) = \frac{K(0)}{mh} \max_{s \in \boldsymbol{a}_m} n_s = KD(\boldsymbol{a}_m, K, h, t),$$

and the uniqueness follows from $n_t > M$.

Case (ii) $[K(t) \to 0$ as $|t| \to \infty$]: By symmetry and continuity, $0 \le K(t) \le K(0)$ for all t, and for every $\varepsilon > 0$ there exists $T_{\varepsilon} < \infty$ such that $\sup_{|t| \ge T_{\varepsilon}} K(t) \le \varepsilon$. Fix small $\varepsilon > 0$ so that

$$\varepsilon < \frac{K(0)}{2m}\gamma. \tag{8}$$

Choose $h_0 > 0$ with $\delta/(2h_0) \ge T_{\varepsilon}$. For any $0 < h \le h_0$ and $x \in \mathbb{R}$, let $s^*(x) \in \boldsymbol{a}_m$ be a nearest element of \boldsymbol{a}_m to x (breaking ties arbitrarily). Points $a_i \ne s^*(x)$ satisfy $|x - a_i| \ge \delta/2$, hence

$$K\left(\frac{x-a_i}{h}\right) \le \sup_{|u| \ge \delta/(2h)} K(u) \le \varepsilon,$$

and thus

$$KD(\boldsymbol{a}_m, K, h, x) \le \frac{n_{s^*(x)}K(0)}{mh} + \frac{(m - n_{s^*(x)})\varepsilon}{mh}.$$
 (9)

Evaluating at x = t gives

$$KD(\boldsymbol{a}_m, K, h, t) \ge \frac{n_t K(0)}{mh} - \frac{(m - n_t)\varepsilon}{mh}.$$
(10)

Combining (9) and (10) with $M = \max_{s \in a_m \neq t} n_s$, $\gamma = n_t - M$ and defining $\mathcal{B}(t, r) = \{x \in a_m \neq t \mid x \in a_m \neq t \}$

 $\mathbb{R}: |x-t| < r\}$, we have for any $x \in \mathbb{R} \setminus \mathcal{B}(t, \delta/2)$:

$$KD(\boldsymbol{a}_{m}, K, h, t) - KD(\boldsymbol{a}_{m}, K, h, x)$$

$$\geq \frac{1}{mh} \left(n_{t}K(0) - (m - n_{t})\varepsilon - MK(0) - (m - M)\varepsilon \right)$$

$$= \frac{1}{mh} \left((n_{t} - M)K(0) - (m + m - n_{t} - M)\varepsilon \right)$$

$$\geq \frac{1}{mh} \left((n_{t} - M)K(0) - 2m\varepsilon \right)$$

$$= \frac{2}{h} \left(\gamma \frac{K(0)}{2m} - \varepsilon \right) > 0^{\circ}$$

$$(11)$$

By the choice (8), the right-hand side is strictly positive.

Now consider the fixed annulus $A := \{x : 0 < |x - t| \le \delta/2\} = \mathcal{B}(t, \delta/2) \setminus \{t\}$. Define $\eta(x,h) := K(0) - K((x-t)/h)$ where $x \in A$. Since K attains its maximum only at x = 0, we have $\eta(x,h) > 0$ for every $x \in A$. moreover $\eta(x,h) \uparrow K(0)$ as $h \downarrow 0$. Thus, decreasing h_0 if needed, ensure that for all $x \in A$,

$$n_t \cdot \eta(x, h) \ge 3(m - n_t)\varepsilon, \forall 0 < h \le h_0.$$
 (12)

hence for any $x \in A$ and $0 < h \le h_0$,

$$KD(\boldsymbol{a}_m, K, h, t) - KD(\boldsymbol{a}_m, K, h, x) \ge \frac{1}{mh} \left(n_t \cdot \eta(x, h) - 2(m - n_t) \varepsilon \right) > 0.$$
 (13)

Now fix any r > 0, since

$$\mathbb{R} \setminus \mathcal{B}(t,r) \subset \left(\mathbb{R} \setminus \mathcal{B}(t,\delta/2) \right) \cup \left\{ x : r \leq |x-t| \leq \delta/2 \right\} \subset \left(\mathbb{R} \setminus \mathcal{B}(t,\delta/2) \right) \cup A,$$

Combining Equations 11–13 yields that for any $0 < h \le h_0$ and $x \in \mathbb{R} \setminus \mathcal{B}(t,r)$, we have:

$$KD(\boldsymbol{a}_m, K, h, t) > KD(\boldsymbol{a}_m, K, h, x),$$

Hence t is the unique global mode in this setup.

S1.3 Proof of Theorem 1

Proof. For the proof of this corollary, we will use a result from Vaart & Wellner (1997) on the convergence of argmax of stochastic processes.

Lemma S1.1. Let M_n be a stochastic process indexed by a metric space Θ , and let M: $\Theta \mapsto \mathbb{R}$ be a deterministic function. Suppose that $\|M_n - M\|_{\Theta}$ in outer probability and that there exists a θ_0 such that

$$M(\theta_0) > \sup_{\theta \notin G} M(\theta)$$

for any open set G that contains θ_0 . Then any sequence $\hat{\theta}_n$, such that $\mathbf{M}_n(\hat{\theta}_n) \geq \sup_{\theta} \mathbf{M}_n(\theta) - o_P(1)$, satisfies $\hat{\theta}_n \to \theta$ in outer probability.

For this proof, first we will show that $||KD(\mathcal{C}_n, K, h, \cdot) - KD(\beta + R_d, K, h, \cdot)||_{\mathbb{R}} \xrightarrow{P} 0$ and then resort to the Argmax Theorem stated in Lemma S1.1 to prove consistency of our mode estimator. First, let us observe that since the kernel K() is assumed to be Lipschitz continuous, then for any $x, y \in \mathbb{R}$ and a constant $L_K > 0$ (dependent on K), we can say $|K(x) - K(y)| \leq L_K |x - y|$. Thus, using this, we have:

$$||KD(\mathcal{C}_{n}, K, h, x) - KD(\beta + R_{d}, X, h, x)||_{\mathbb{R}}$$

$$= \sup_{x \in \mathbb{R}} |KD(\mathcal{C}_{n}, K, x) - KD(\beta + R_{d}, K, x)|$$

$$= \sup_{x \in \mathbb{R}} \left| \frac{1}{mh} \sum_{k \in S_{x,d}} K\left(\frac{x - \hat{\beta}_{k,n}}{h}\right) - \frac{1}{mh} \sum_{k \in S_{x,d}} K\left(\frac{x - (\beta + r_{k,d})}{h}\right) \right|$$

$$\leq \sup_{x \in \mathbb{R}} \frac{1}{mh} \sum_{k \in S_{x,d}} |K\left(\frac{x - \hat{\beta}_{k,n}}{h}\right) - K\left(\frac{x - (\beta + r_{k,d})}{h}\right)|$$

$$\leq \sup_{x \in \mathbb{R}} \frac{L_{K}}{mh} \sum_{k \in S_{x,d}} \left| \left(\frac{x - \hat{\beta}_{k,n}}{h}\right) - \left(\frac{x - (\beta + r_{k,d})}{h}\right) \right| \quad \text{(using Lipschitz Continuity)}$$

$$= \frac{L_{K}}{mh^{2}} \sum_{k \in S_{x,d}} \left| \hat{\beta}_{k,n} - (\beta + r_{k,d}) \right| \xrightarrow{P} 0$$

This last step is because $\frac{L_K}{mh^2} < \infty$ and $|S_{x,d}| = m$, which is fixed, and each of the summands

goes to 0 in probability as per the assumption of the theorem. Hence, we have the desired result for the sup-norm of the difference of the KD's.

Now, based on the Plurality Rule Assumption 2, and Lemma 1, it is ensured that for $\theta_0 = \beta$, we have $KD(\beta, K, h, \theta_0) > \sup_{\theta \notin G} KD(\theta + R_d, K, h, \theta)$ for any open set G that contains θ_0 .

Thus defining $\hat{\beta}_n = \underset{x}{\operatorname{arg\,max}} KD(\mathcal{C}_n, K, h, x)$, we can say that $KD\left(\mathcal{C}_n, K, h, \hat{\beta}_n\right) \geq \sup_{\theta} KD\left(\mathcal{C}_n, K, h, \theta\right) - o_P(1)$. Thus, using Lemma S1.1, we can say that $\hat{\beta}_n \xrightarrow{P} \beta$.

Before starting the proof for the next theorems, we will state a few Lemmas which will have the building blocks that we will be needing for the proof:

Lemma S1.2. For any basis function h_j from the orthogonal class \mathcal{H} , defining its evaluation at coordinates $S_1, S_2, \dots, S_n \stackrel{iid}{\sim} f_S > 0$ as $\boldsymbol{h}_{n,j} = (h_j(S_1), \dots, h_j(S_n))^{\top}$ and for iid noise vector $\boldsymbol{\zeta}_n = (\zeta_1, \dots, \zeta_n) \sim N(\boldsymbol{0}, \sigma_{\zeta}^2 \boldsymbol{I}_n)$ where $\boldsymbol{\zeta}_n \perp \boldsymbol{S}_n = (S_1, \dots, S_n)^{\top}$, the following holds:

1.
$$\frac{1}{n} \mathbf{h}_{n,j}^{\top} \mathbf{h}_{n,l} \xrightarrow[n \to \infty]{P} \mathbb{I}(j=l)$$
 where $\mathbb{I}(\cdot)$ is the indicator function for any $j, l \geq 1$

2.
$$\frac{1}{n} \boldsymbol{h}_{n,j}^{\top} \boldsymbol{\zeta}_n \xrightarrow[n \to \infty]{P} 0 \text{ for any } j \geq 1$$

Proof. Consider the fact that the basis function set $\mathcal{H} = \{h_k(\cdot) : \int_{\mathcal{D}} h_i(s)h_j(s)f_S(s)ds = \delta_{ij}\}$ where $\delta_{ij} = 1$ iff i = j. Now, this Lemma follows trivially from the Weak Law of Large Numbers (WLLN). To show 1, notice that:

$$\frac{1}{n}\boldsymbol{h}_{n,j}^{\top}\boldsymbol{h}_{n,l} = \frac{1}{n}\sum_{i=1}^{n}h_{j}(s_{i})h_{l}(s_{i}) \xrightarrow[n \to \infty]{P} \mathbb{E}h_{j}(S_{1})h_{l}(S_{1}) = \int h_{j}(s)h_{l}(s)f_{S}(s)ds = \mathbb{I}(j=l)$$

Now, to see 2, observe that:

$$\mathbb{E}rac{1}{n}oldsymbol{h}_{n,j}^{ op}oldsymbol{\zeta}_n = \mathbb{E}_{oldsymbol{S}_n}rac{1}{n}oldsymbol{h}_{n,j}^{ op}\mathbb{E}_{oldsymbol{\zeta}_n|oldsymbol{S}_n}\left[oldsymbol{\zeta}_n|oldsymbol{S}_n
ight] = \mathbb{E}_{oldsymbol{S}_n}rac{1}{n}oldsymbol{h}_{n,j}^{ op}\mathbb{E}_{oldsymbol{\zeta}_n|oldsymbol{S}_n}\left[oldsymbol{\zeta}_n
ight] = oldsymbol{0}$$

Also, observe that:

$$Var\left(\boldsymbol{h}_{n,j}^{\top}\boldsymbol{\zeta}_{n}\right) = Var_{\boldsymbol{S}_{n}}\mathbb{E}[\boldsymbol{h}_{n,j}^{\top}\boldsymbol{\zeta}_{n}|\boldsymbol{S}_{n}] + \mathbb{E}_{\boldsymbol{S}_{n}}Var[\boldsymbol{h}_{n,j}^{\top}\boldsymbol{\zeta}_{n}|\boldsymbol{S}_{n}]$$

$$= \mathbb{E}_{\boldsymbol{S}_{n}}Var[\boldsymbol{h}_{n,j}^{\top}\boldsymbol{\zeta}_{n}|\boldsymbol{S}_{n}]$$

$$= \sigma_{\zeta}^{2}\mathbb{E}_{\boldsymbol{S}_{n}}\boldsymbol{h}_{n,j}^{\top}\boldsymbol{h}_{n,j} = n\sigma_{\zeta}^{2}\mathbb{E}\boldsymbol{h}_{j}^{2}(\boldsymbol{S}_{1})$$

$$= n\sigma_{\zeta}^{2}\int_{\mathcal{D}}\boldsymbol{h}_{j}^{2}(\boldsymbol{s})f_{\boldsymbol{S}}(\boldsymbol{s})d\boldsymbol{s} = n\sigma_{\zeta}^{2}$$

$$\implies Var\left(\frac{1}{n}\boldsymbol{h}_{n,j}^{\top}\boldsymbol{\zeta}_{n}\right) = \frac{\sigma_{\zeta}^{2}}{n} \xrightarrow{n \to \infty} 0$$

This shows that $\frac{1}{n} \boldsymbol{h}_{n,j}^{\top} \boldsymbol{\zeta}_n \xrightarrow{P} 0$ and this completes the proof of Lemma S1.2.

S1.4 Proof of Theorem 2

Proof. Recall that $\boldsymbol{H}_{1:d} = \begin{bmatrix} \boldsymbol{h}_{n,1} & \dots & \boldsymbol{h}_{n,d} \end{bmatrix}$ and \boldsymbol{P}_d is the projection matrix on its column space. Let us choose some $j \in S_{x,d}$, which means $\alpha_x^{(j)} \neq 0$. Now, let us look at $\hat{\beta}_{j,n}^{PROJ}$:

$$\hat{\beta}_{j,n}^{PROJ} = \frac{\frac{1}{n} \boldsymbol{h}_{n,j}^{\top} \boldsymbol{Y}_{n}}{\frac{1}{n} \boldsymbol{h}_{n,j}^{\top} \boldsymbol{X}_{n}} = \frac{\frac{1}{n} \boldsymbol{h}_{n,j}^{\top} (\beta \boldsymbol{X}_{n} + \boldsymbol{U}_{n} + \boldsymbol{\epsilon}_{n})}{\frac{1}{n} \boldsymbol{h}_{n,j}^{\top} \boldsymbol{X}_{n}}$$
$$= \beta + \frac{\frac{1}{n} \boldsymbol{h}_{n,j}^{\top} \boldsymbol{U}_{n}}{\frac{1}{n} \boldsymbol{h}_{n,j}^{\top} \boldsymbol{X}_{n}} + \frac{\frac{1}{n} \boldsymbol{h}_{n,j}^{\top} \boldsymbol{\epsilon}_{n}}{\frac{1}{n} \boldsymbol{h}_{n,j}^{\top} \boldsymbol{X}_{n}}$$

where we have $X_n = \sum_{k=1}^{\infty} \alpha_x^{(k)} h_{n,k}$ and $U_n = \sum_{k=1}^{\infty} \alpha_u^{(k)} h_{n,k}$. By WLLN, $\frac{1}{n} h_{n,j}^{\top} X_n \xrightarrow{P} \mathbb{I}_{n \to \infty} \mathbb{I}_{n \to \infty}$

 $s \in \mathcal{D}$ and we have:

$$\mathbb{E}h_{j}(S)X_{k}(S) = \int h_{j}(s)X_{k}(s)f_{S}ds$$

$$= \sum_{u=1}^{k} \alpha_{x}^{(u)} \int h_{j}(s)h_{u}(s)f_{S}ds$$

$$= \sum_{u=1}^{k} \alpha_{x}^{(u)}\mathbb{I}(u=j)$$

$$\leq \sup_{u \geq 1} \alpha_{x}^{(u)} \sum_{u=1}^{k} \mathbb{I}(u=j) \leq \sup_{u \geq 1} \alpha_{x}^{(u)} \leq \sum_{u \geq 1} \alpha_{x}^{(u)^{2}} < \infty$$

Thus Dominated Convergence Theorem (DCT) implies that:

$$\mathbb{E}h_j(S)X_k(S) \xrightarrow{k \to \infty} \mathbb{E}h_j(S)X(S) = \sum_{u=1}^{\infty} \alpha_x^{(u)} \mathbb{I}(u=j) = \alpha_x^{(j)}$$

Similarly we have $\frac{1}{n}\boldsymbol{h}_{n,j}^{\top}\boldsymbol{U}_n \xrightarrow{P} \alpha_u^{(j)}$. Lemma S1.2 implies that $\frac{1}{n}\boldsymbol{h}_{n,j}^{\top}\boldsymbol{\epsilon}_n \xrightarrow{P} 0$. Thus for $j \in S_{x,d}$ i.e. when $\alpha_x^{(j)} \neq 0$, we have $\hat{\beta}_{j,n}^{PROJ} \xrightarrow{P} \beta + \alpha_u^{(j)}/\alpha_x^{(j)} = \beta + r_{j,d}$ which completes the proof of consistency. Let us define $A_i = h_j(S_i)[U(S_i) + \epsilon_i]$ and $B_n = h_j(S_i)X(S_i)$, which means $\frac{1}{n}\boldsymbol{h}_{n,j}^{\top}[\boldsymbol{U}_n + \boldsymbol{\epsilon}_n] = \frac{1}{n}\sum_{i=1}^n h_j(S_i)[U(S_i) + \epsilon_i] = \bar{A}_n$ and $\frac{1}{n}\boldsymbol{h}_{n,j}^{\top}\boldsymbol{X}_n = \frac{1}{n}\sum_{i=1}^n h_j(S_i)X(S_i) = \bar{B}_n$. We will try to derive the asymptotic distribution of \bar{A}_n/\bar{B}_n , which is the bias of the estimator $\hat{\beta}_{j,n}^{PROJ}$. Now we have seen that $\mathbb{E}A_i = \mathbb{E}h_j(S_i)[U(S_i) + \epsilon_i] = \mathbb{E}h_j(S_i)U(S_i) = \int h_j(s)U(s)f_s(s)ds = \alpha_u^{(j)}$ and $\mathbb{E}B_i = \mathbb{E}h_j(S_i)X(S_i) = \alpha_x^{(j)}$ Also, notice that

$$\mathbb{E}A_i^2 = \mathbb{E}\left[h_j^2(S_i)(U(S_i) + \epsilon_i)^2\right]$$

$$= \mathbb{E}[h_j(S_i)U(S_i)]^2 + \mathbb{E}\left[h_j^2(S_i)\epsilon_i^2\right] + 2\mathbb{E}[h_j(S_i)U(S_i)\epsilon_i]$$

$$= \int [h_j(s)U(s)]^2 f_S(s) \, ds + \sigma_\epsilon^2$$

$$= \|h_j U\|_{f_S}^2 + \sigma_\epsilon^2$$

And similarly, we will have $\mathbb{E}B_i^2 = \int [h_j(s)X(s)]^2 f_S(s) ds = ||h_jX||_{f_S}^2$. Also, note that:

$$\mathbb{E}A_i B_i = \mathbb{E}[h_j(S)(U(S) + \epsilon_i)h_j(S)X(S)]$$
$$= \int h_j^2(s)U(s)X(s)f_S(s) ds$$

Since $\int (h_j U(s))^2 f_S ds < \infty$ and $\int (h_j X(s))^2 f_S ds < \infty$ as the functions are elements of $\mathcal{L}^4(\mathcal{D}, f_S)$, by Multivariate Central Limit Theorem (CLT), we have:

$$\sqrt{n} \left\{ \begin{pmatrix} \bar{A}_n \\ \bar{B}_n \end{pmatrix} - \begin{pmatrix} \alpha_u^{(j)} \\ \alpha_x^{(j)} \end{pmatrix} \right\} = \frac{1}{\sqrt{n}} \sum_{i=1}^n \left\{ \begin{pmatrix} A_i \\ B_i \end{pmatrix} - \begin{pmatrix} \alpha_u^{(j)} \\ \alpha_x^{(j)} \end{pmatrix} \right\} \xrightarrow[n \to \infty]{} N\left(\mathbf{0}_2, \mathbf{\Sigma}_{AB}\right) \tag{14}$$

where $\mathbf{0}_2 = (0,0)^{\top}$, and $\mathbf{\Sigma}_{AB} = \begin{pmatrix} \sigma_{\epsilon}^2 + \sigma_{U,j}^2 & \sigma_{U,X,j} \\ \sigma_{U,X,j} & \sigma_{X,j}^2 \end{pmatrix}$ with:

$$\sigma_{U,j}^{2} = \int (h_{j}(s)U(s))^{2} f_{S}(s) ds - \alpha_{u}^{(j)^{2}} = \|h_{j}U\|_{f_{S}}^{2} - \alpha_{u}^{(j)^{2}}$$

$$\sigma_{X,j}^{2} = \int (h_{j}(s)X(s))^{2} f_{S}(s) ds - \alpha_{x}^{(j)^{2}} = \|h_{j}X\|_{f_{S}}^{2} - \alpha_{x}^{(j)^{2}}$$

$$\sigma_{U,X,j} = \int h_{j}^{2}(s)X(s)U(s) f_{S}(s) ds - \alpha_{x}^{(j)}\alpha_{u}^{(j)} = \langle h_{j}X, h_{j}U \rangle_{f_{S}} - \alpha_{u}^{(j)}\alpha_{x}^{(j)}$$

Now, using Delta Method on the bivariate function $g:(x,y)\mapsto x/y$, defining $\nabla g=\left(\frac{1}{\alpha_x^{(j)}},-\frac{\alpha_u^{(j)}}{\alpha_x^{(j)^2}}\right)^{\top}$, we have:

$$\sqrt{n} \left(\frac{\bar{A}_n}{\bar{B}_n} - \underbrace{\frac{\alpha_u^{(j)}}{\alpha_x^{(j)}}}_{r_{j,d}} \right) \xrightarrow[n \to \infty]{d} N\left(0, \sigma_{j,d}^2\right)$$
(15)

where:

$$\sigma_{j,d}^{2} = \nabla g^{\top} \mathbf{\Sigma}_{AB} \nabla g = \frac{\sigma_{U,j}^{2} + \sigma_{\epsilon}^{2}}{\alpha_{x}^{(j)^{2}}} + \left(\frac{\alpha_{u}^{(j)}}{\alpha_{x}^{(j)^{2}}}\right)^{2} \sigma_{X,j}^{2} - 2\frac{\alpha_{u}^{(j)}}{\alpha_{x}^{(j)^{3}}} \sigma_{U,X,j}$$
$$= \frac{\sigma_{U,j}^{2} + \sigma_{\epsilon}^{2}}{\alpha_{x}^{(j)^{2}}} + \alpha_{u}^{(j)} \left(\frac{\alpha_{u}^{(j)}}{\alpha_{x}^{(j)^{4}}} \sigma_{X,j}^{2} - \frac{2}{\alpha_{x}^{(j)^{3}}} \sigma_{U,X,j}\right)$$

Thus, if $j \in O_X$, then $\alpha_u^{(j)} = 0$ and thus $r_{j,d} = 0$, which means $\sigma_{j,d}^2 = \frac{\sigma_{U,j}^2 + \sigma_{\epsilon}^2}{\alpha_x^{(j)^2}}$. Thus for such a $j \in O_X$, we have:

$$\sqrt{n} \left(\hat{\beta}_{j,n}^{PROJ} - \beta \right) \xrightarrow[n \to \infty]{d} N \left(0, \frac{\sigma_{U,j}^2 + \sigma_{\epsilon}^2}{\alpha_x^{(j)^2}} \right)$$

This completes the proof of Theorem 2 and also proves Corollary 1.

S1.5 Proof of Theorem 3

Proof. Recall the notations that we will be using for the proof:

$$egin{aligned} oldsymbol{H}_{1:d} &= egin{bmatrix} oldsymbol{h}_{n,1} & \cdots & oldsymbol{h}_{n,d} \end{bmatrix} \ oldsymbol{H}_{-j|1:d} &= egin{bmatrix} oldsymbol{h}_{n,1} & \cdots & oldsymbol{h}_{n,j-1} & oldsymbol{h}_{n,j+1} & \cdots & oldsymbol{h}_{n,d} \end{bmatrix} \ oldsymbol{P}_{d} &= oldsymbol{H}_{1:d} \left(oldsymbol{H}_{1:d}^{ op} oldsymbol{H}_{1:d}
ight)^{-1} oldsymbol{H}_{1:d}^{ op} \ oldsymbol{H}_{-j|1:d} & oldsymbol{H}_{-j|1:d} \ oldsymbol{X}_{d,n} &= oldsymbol{H}_{d} oldsymbol{X}_{n} \ oldsymbol{Y}_{d,n} &= oldsymbol{P}_{d} oldsymbol{Y}_{n} \end{aligned}$$

We will simplify certain notations $H_{1:d} \to H_d$ and $H_{-j|1:d} \to H_{-j,d}$. Using these notations, we define out drop-one estimator for $j \in S_{x,d}$ can be simplified as:

$$\begin{split} \hat{\beta}_{-j,n} = & \frac{\boldsymbol{X}_{d,n}^{\top}(\boldsymbol{I}_n - \boldsymbol{P}_{-j,d})\boldsymbol{Y}_{d,n}}{\boldsymbol{X}_{d,n}^{\top}(\boldsymbol{I}_n - \boldsymbol{P}_{-j,d})\boldsymbol{X}_{k,d}} \\ = & \frac{\boldsymbol{X}_n^{\top}\boldsymbol{P}_d(\boldsymbol{I}_n - \boldsymbol{P}_{-j,d})\boldsymbol{P}_d\boldsymbol{Y}_n}{\boldsymbol{X}_n^{\top}\boldsymbol{P}_d(\boldsymbol{I}_n - \boldsymbol{P}_{-j,d})\boldsymbol{P}_d\boldsymbol{X}_n} \\ = & \frac{\boldsymbol{X}_n^{\top}\boldsymbol{P}_d(\boldsymbol{I}_n - \boldsymbol{P}_{-j,d})\boldsymbol{P}_d(\boldsymbol{X}_n\boldsymbol{\beta} + \boldsymbol{U}_n + \boldsymbol{\epsilon}_n)}{\boldsymbol{X}_n^{\top}\boldsymbol{P}_d(\boldsymbol{I}_n - \boldsymbol{P}_{-j,d})\boldsymbol{P}_d\boldsymbol{X}_n} \\ = & \boldsymbol{\beta} + \frac{\boldsymbol{X}_n^{\top}\boldsymbol{P}_d(\boldsymbol{I}_n - \boldsymbol{P}_{-j,d})\boldsymbol{P}_d(\boldsymbol{U}_n + \boldsymbol{\epsilon}_n)}{\boldsymbol{X}_n^{\top}\boldsymbol{P}_d(\boldsymbol{I}_n - \boldsymbol{P}_{-j,d})\boldsymbol{P}_d\boldsymbol{X}_n} \end{split}$$

Notice that:

$$\frac{1}{n} \mathbf{P}_{d} (\mathbf{I}_{n} - \mathbf{P}_{-j,d}) \mathbf{P}_{d}
= \frac{1}{n} \mathbf{H}_{d} \left(\mathbf{H}_{d}^{\top} \mathbf{H}_{d} \right)^{-1} \mathbf{H}_{d}^{\top} (\mathbf{I}_{n} - \mathbf{P}_{-j,d}) \mathbf{H}_{d} \left(\mathbf{H}_{d}^{\top} \mathbf{H}_{d} \right)^{-1} \mathbf{H}_{d}^{\top}
= \frac{1}{n} \mathbf{H}_{d} \left(\mathbf{H}_{d}^{\top} \mathbf{H}_{d} \right)^{-1} \mathbf{H}_{d}^{\top} \left(\mathbf{I}_{n} - \mathbf{H}_{-j,d} \left(\mathbf{H}_{-j,d}^{\top} \mathbf{H}_{-j,d} \right)^{-1} \mathbf{H}_{-j,d}^{\top} \right) \mathbf{H}_{d} \left(\mathbf{H}_{d}^{\top} \mathbf{H}_{d} \right)^{-1} \mathbf{H}_{d}^{\top}
= \frac{1}{n} \mathbf{H}_{d} \left(\frac{1}{n} \mathbf{H}_{d}^{\top} \mathbf{H}_{d} \right)^{-1} \left(\frac{1}{n} \mathbf{H}_{d}^{\top} \mathbf{H}_{d} - \frac{1}{n} \mathbf{H}_{d}^{\top} \mathbf{H}_{-j,d} \left(\frac{1}{n} \mathbf{H}_{-j,d}^{\top} \mathbf{H}_{-j,d} \right)^{-1} \frac{1}{n} \mathbf{H}_{-j,d}^{\top} \mathbf{H}_{d} \right) \left(\frac{1}{n} \mathbf{H}_{d}^{\top} \mathbf{H}_{d} \right)^{-1} \underbrace{1}_{n} \mathbf{H}_{d}^{\top}
= \frac{1}{n} \mathbf{H}_{d} \mathbf{A}_{j,d} \frac{1}{n} \mathbf{H}_{d}^{\top}
= \frac{1}{n} \mathbf{H}_{d} \mathbf{A}_{j,d} \frac{1}{n} \mathbf{H}_{d}^{\top}$$

(16)

Next we prove a lemma about the probability limit of $A_{j,d}$:

Lemma S1.3. For the $d \times d$ matrix $A_{j,d}$ defined in Equation 16, we have:

•
$$A_{j,d} \xrightarrow[n \to \infty]{P} A_{j,d}^{lim} := diag(\{\mathbb{I}(u=j), 1 \le u \le d\})$$

•
$$\left\| \sqrt{n} \left(\mathbf{A}_{j,d} - \mathbf{A}_{j,d}^{lim} \right) \right\|_2 = \mathcal{O}_P(1)$$
 where $|| \cdot ||_2$ denotes the spectral norm.

Proof. Using Lemma S1.2, we can say that $\frac{1}{n} \boldsymbol{H}_d^{\top} \boldsymbol{H}_d \xrightarrow{P} \boldsymbol{I}_d$ and $\frac{1}{n} \boldsymbol{H}_{-j,d}^{\top} \boldsymbol{H}_{-j,d} \xrightarrow{P} \boldsymbol{I}_{d-1}$, and similarly using the same lemma, we can say that:

$$\frac{1}{n}\boldsymbol{H}_{-j,d}^{\top}\boldsymbol{H}_{d} = \frac{1}{n} \begin{bmatrix} \boldsymbol{h}_{n,1}^{\top} \\ \boldsymbol{h}_{n,j-1}^{\top} \\ \boldsymbol{h}_{n,j+1}^{\top} \\ \vdots \\ \boldsymbol{h}_{n,d}^{\top} \end{bmatrix} \begin{bmatrix} \boldsymbol{h}_{n,1} & \cdots & \boldsymbol{h}_{n,j-1} & \boldsymbol{h}_{n,j} & \boldsymbol{h}_{n,j+1} & \cdots & \boldsymbol{h}_{n,d} \end{bmatrix}$$

$$= \frac{1}{n} \begin{bmatrix} \boldsymbol{H}_{1:(j-1),n}^{\top} \\ \boldsymbol{H}_{(j+1):d,n}^{\top} \end{bmatrix}_{(d-1)\times n} \begin{bmatrix} \boldsymbol{H}_{1:(j-1),n} & \boldsymbol{h}_{n,j} & \boldsymbol{H}_{(j+1):d,n} \end{bmatrix}_{n\times d}$$

$$\xrightarrow{P} \begin{cases} \boldsymbol{I}_{j-1} & \boldsymbol{0}_{j-1} & \boldsymbol{0}_{(j-1)\times(d-j)} \\ \boldsymbol{0}_{(d-j)\times(j-1)} & \boldsymbol{0}_{d-j} & \boldsymbol{I}_{d-j} \end{bmatrix} = \boldsymbol{R}_{j,d}$$

$$(17)$$

with:

$$\boldsymbol{R}_{j,d}^{\top} \boldsymbol{R}_{j,d} = \begin{vmatrix} \boldsymbol{I}_{j-1} & \boldsymbol{0}_{j-1} & \boldsymbol{0}_{(j-1)\times(d-j)} \\ \boldsymbol{0}_{j-1}^{\top} & 0 & \boldsymbol{0}_{d-j} \\ \boldsymbol{0}_{(d-j)\times(j-1)} & \boldsymbol{0}_{d-j} & \boldsymbol{I}_{d-j} \end{vmatrix}$$
(18)

Hence, we have:

$$\mathbf{A}_{j,d} = \left(\frac{1}{n}\mathbf{H}_{d}^{\top}\mathbf{H}_{d}\right)^{-1} \left(\frac{1}{n}\mathbf{H}_{d}^{\top}\mathbf{H}_{d} - \frac{1}{n}\mathbf{H}_{d}^{\top}\mathbf{H}_{-j,d} \left(\frac{1}{n}\mathbf{H}_{-j,d}^{\top}\mathbf{H}_{-j,d}\right)^{-1} \frac{1}{n}\mathbf{H}_{-j,d}^{\top}\mathbf{H}_{d}\right) \left(\frac{1}{n}\mathbf{H}_{d}^{\top}\mathbf{H}_{d}\right)^{-1}$$

$$\xrightarrow{P} \mathbf{I}_{d}^{-1} \left(\mathbf{I}_{d} - R_{j,d}^{\top}\mathbf{I}_{d-1}^{-1}R_{j,d}\right) \mathbf{I}_{d}^{-1}$$

$$= \mathbf{I}_{d} - \begin{bmatrix} \mathbf{I}_{j-1} & \mathbf{0}_{j-1} & \mathbf{0}_{(j-1)\times(d-j)} \\ \mathbf{0}_{j-1}^{\top} & 0 & \mathbf{0}_{d-j} \\ \mathbf{0}_{(d-j)\times(j-1)} & \mathbf{0}_{d-j} & \mathbf{I}_{d-j} \end{bmatrix} = diag(\{\mathbb{I}(u=j), 1 \leq u \leq d\}) = \mathbf{A}_{j,d}^{lim}$$

This completes the proof of the first part lemma. Next, we move to proving the uniform tightness of a matrix deviation. Before that, we prove something very general:

Proposition 1. Let \mathbf{A}_n be a $k \times k$ finite dimensional matrix of the form $\mathbf{A}_n = \frac{1}{n} \sum_{l=1}^n A_\ell$ such that each of A_ℓ are iid square matrices of dimension k such that $\mathbb{E}A_\ell = \mathbf{A}$ with $||\mathbf{A}||_2 < \infty$. Then we have:

$$\left\| \sqrt{n} \left(\boldsymbol{A}_n^{-1} - \boldsymbol{A}^{-1} \right) \right\|_2 = \mathcal{O}_P(1)$$

where $||\cdot||_2$ is the spectral norm.

Proof. From Central Limit Theorem for matrices, we can say that the scaled difference $\sqrt{n} (\mathbf{A}_n - \mathbf{A}) \xrightarrow[n \to \infty]{d} \mathbf{Z}$ where \mathbf{Z} is a matrix normal random variable with mean matrix to be a square $\mathbf{0}$ matrix of dimension k and covariance matrix same as the covariance of $vec(A_l)$, and since $||\cdot||_2$ is a continuous function on matrices, thus we can say that

 $||\sqrt{n}(\boldsymbol{A}_n-\boldsymbol{A})||_2=\mathcal{O}_P(1)$. Defining $\boldsymbol{\Delta}_n=\boldsymbol{A}_n-\boldsymbol{A}$, we have:

$$egin{aligned} & m{A}_n^{-1} = & (m{A}_n + m{A} - m{A})^{-1} \ & = & (m{A} + m{\Delta}_n)^{-1} \ & = & m{A}^{-1} \left(m{I} + m{\Delta}_n m{A}^{-1}
ight)^{-1} \ & = & m{A}^{-1} \sum_{k \geq 0} \left(-m{\Delta}_n m{A}^{-1}
ight)^k \ & = & m{A}^{-1} - m{A}^{-1} m{\Delta}_n m{A}^{-1} + m{A}^{-1} \left(-m{\Delta}_n m{A}^{-1}
ight)^2 + m{A}^{-1} \left(-m{\Delta}_n m{A}^{-1}
ight)^3 + \cdots \ & = & m{A}^{-1} - m{A}^{-1} m{\Delta}_n m{A}^{-1} + \mathcal{O} \left(||m{\Delta}_n||_2^2 \right) \end{aligned}$$

Now, as $||\sqrt{n}\Delta_n||_2 = \mathcal{O}_P(1)$, it implies that $\sqrt{n}||\Delta_n||_2^2 = \mathcal{O}_P(n^{-1/2}) = o_P(1)$. Thus, we have:

$$\left\| \sqrt{n} (\boldsymbol{A}_n^{-1} - \boldsymbol{A}^{-1}) \right\|_2 \le \|\boldsymbol{A}^{-1}\|_2^2 \|\sqrt{n} \boldsymbol{\Delta}_n\|_2 + \mathcal{O}_P(\sqrt{n} ||\boldsymbol{\Delta}_n||_2^2) = \mathcal{O}_P(1)$$

This completes the proof of the proposition.

We will be using this result in proving the second part of our lemma. Recall how We defined the matrix $A_{j,d}$ as:

$$A_{j,d} = \left(\frac{1}{n}\boldsymbol{H}_d^{\top}\boldsymbol{H}_d\right)^{-1} \left(\frac{1}{n}\boldsymbol{H}_d^{\top}\boldsymbol{H}_d - \frac{1}{n}\boldsymbol{H}_d^{\top}\boldsymbol{H}_{-j,d} \left(\frac{1}{n}\boldsymbol{H}_{-j,d}^{\top}\boldsymbol{H}_{-j,d}\right)^{-1} \frac{1}{n}\boldsymbol{H}_{-j,d}^{\top}\boldsymbol{H}_d\right) \left(\frac{1}{n}\boldsymbol{H}_d^{\top}\boldsymbol{H}_d\right)^{-1}.$$

and its probability limit $A_{j,d}^{lim} = \text{diag}(\mathbb{I}(u=j), 1 \le u \le d)$ which is a $d \times d$ matrix with 1 at position (j,j) and 0 elsewhere. Let us define:

$$M_{n} := \frac{1}{n} \boldsymbol{H}_{d}^{\top} \boldsymbol{H}_{d} \xrightarrow{P} \boldsymbol{I}_{d}$$

$$\boldsymbol{C}_{n}^{\top} := \frac{1}{n} \boldsymbol{H}_{d}^{\top} \boldsymbol{H}_{-j,d} \xrightarrow{P} \boldsymbol{R}_{j,d}^{\top} \text{ (Eqn. 17)}$$

$$\boldsymbol{D}_{n} := \frac{1}{n} \boldsymbol{H}_{-j,d}^{\top} \boldsymbol{H}_{-j,d} \xrightarrow{P} \boldsymbol{I}_{d-1}$$

Then,

$$\boldsymbol{A}_{j,d} = \boldsymbol{M}_n^{-1} \left(\boldsymbol{M}_n - \boldsymbol{C}_n^\top \boldsymbol{D}_n^{-1} \boldsymbol{C}_n \right) \boldsymbol{M}_n^{-1} = \boldsymbol{M}_n^{-1} - \boldsymbol{M}_n^{-1} \boldsymbol{C}_n^\top \boldsymbol{D}_n^{-1} \boldsymbol{C}_n \boldsymbol{M}_n^{-1}$$

Also, observe that we can write down $A_{j,d}^{lim} = I_d - R_{j,d}^{\top} R_{j,d}$ where $R_{j,d}^{\top} R_{j,d}$ has all the diagonal entries to be 1 except the j-th diagonal element which is 0 as seen in Equation 18. We denote $R_{j,d}^* := R_{j,d}^{\top} R_{j,d}$. Thus, we have:

$$\sqrt{n} \left(\mathbf{A}_{j,d} - \mathbf{A}_{j,d}^{lim} \right)
= \sqrt{n} \left[\left(\mathbf{M}_{n}^{-1} - \mathbf{I}_{d} \right) - \left(\mathbf{M}_{n}^{-1} \mathbf{C}_{n}^{\top} \mathbf{D}_{n}^{-1} \mathbf{C}_{n} \mathbf{M}_{n}^{-1} - \mathbf{R}_{j,d}^{*} \right) \right]
= \sqrt{n} \left(\mathbf{M}_{n}^{-1} - \mathbf{I}_{d} \right) - \sqrt{n} \left[\mathbf{M}_{n}^{-1} (\mathbf{C}_{n}^{\top} \mathbf{D}_{n}^{-1} \mathbf{C}_{n} - \mathbf{R}_{j,d}^{*} + \mathbf{R}_{j,d}^{*}) \mathbf{M}_{n}^{-1} - \mathbf{R}_{j,d}^{*} \right]
= \sqrt{n} \left(\mathbf{M}_{n}^{-1} - \mathbf{I}_{d} \right)
- \mathbf{M}_{n}^{-1} \sqrt{n} \left(\mathbf{C}_{n}^{\top} \mathbf{D}_{n}^{-1} \mathbf{C}_{n} - \mathbf{R}_{j,d}^{*} \right) \mathbf{M}_{n}^{-1}
- \sqrt{n} \left(\mathbf{M}_{n}^{-1} \mathbf{R}_{j,d}^{*} \mathbf{M}_{n}^{-1} - \mathbf{R}_{j,d}^{*} \right)
= \sqrt{n} \left(\mathbf{M}_{n}^{-1} - \mathbf{I}_{d} \right)
- \mathbf{M}_{n}^{-1} \left[\mathbf{C}_{n}^{\top} \sqrt{n} (\mathbf{D}_{n}^{-1} - \mathbf{I}_{d-1}) \mathbf{C}_{n} + \sqrt{n} (\mathbf{C}_{n}^{\top} \mathbf{C}_{n} - \mathbf{R}_{j,d}^{*}) \right] \mathbf{M}_{n}^{-1}
- \sqrt{n} \left[(\mathbf{M}_{n}^{-1} - \mathbf{I}_{d} + \mathbf{I}_{d}) \mathbf{R}_{j,d}^{*} (\mathbf{M}_{n}^{-1} - \mathbf{I}_{d} + \mathbf{I}_{d}) - \mathbf{R}_{j,d}^{*} \right]
= \sqrt{n} \left(\mathbf{M}_{n}^{-1} - \mathbf{I}_{d} \right)
- \mathbf{M}_{n}^{-1} \left[\mathbf{C}_{n}^{\top} \sqrt{n} (\mathbf{D}_{n}^{-1} - \mathbf{I}_{d-1}) \mathbf{C}_{n} + \sqrt{n} (\mathbf{C}_{n}^{\top} \mathbf{C}_{n} - \mathbf{R}_{j,d}^{*}) \right] \mathbf{M}_{n}^{-1}
- \left[\sqrt{n} (\mathbf{M}_{n}^{-1} - \mathbf{I}_{d}) \mathbf{R}_{j,d}^{*} (\mathbf{M}_{n}^{-1} - \mathbf{I}_{d}) + \sqrt{n} (\mathbf{M}_{n}^{-1} - \mathbf{I}_{d}) \mathbf{R}_{j,d}^{*} + \mathbf{R}_{j,d}^{*} \sqrt{n} (\mathbf{M}_{n}^{-1} - \mathbf{I}_{d}) \right]$$

Unless otherwise specified, we will refer to $||\cdot||$ as the spectral norm for matrices. Thus,

using these simplifications, we have:

$$\begin{aligned} & \left\| \sqrt{n} \left(\boldsymbol{A}_{j,d} - \boldsymbol{A}_{j,d}^{lim} \right) \right\|_{2} \\ & \leq \left\| \left\| \sqrt{n} \left(\boldsymbol{M}_{n}^{-1} - \boldsymbol{I}_{d}^{-1} \right) \right\|_{2} \\ & + \left\| \boldsymbol{M}_{n}^{-1} \left[\boldsymbol{C}_{n}^{\top} \sqrt{n} (\boldsymbol{D}_{n}^{-1} - \boldsymbol{I}_{d-1}^{-1}) \boldsymbol{C}_{n} + \sqrt{n} (\boldsymbol{C}_{n}^{\top} \boldsymbol{C}_{n} - \boldsymbol{R}_{j,d}^{*}) \right] \boldsymbol{M}_{n}^{-1} \right\|_{2} \\ & + \left\| \left[\sqrt{n} (\boldsymbol{M}_{n}^{-1} - \boldsymbol{I}_{d}^{-1}) \boldsymbol{R}_{j,d}^{*} (\boldsymbol{M}_{n}^{-1} - \boldsymbol{I}_{d}^{-1}) + \sqrt{n} (\boldsymbol{M}_{n}^{-1} - \boldsymbol{I}_{d}^{-1}) \boldsymbol{R}_{j,d}^{*} + \boldsymbol{R}_{j,d}^{*} \sqrt{n} (\boldsymbol{M}_{n}^{-1} - \boldsymbol{I}_{d}^{-1}) \right] \right\|_{2} \\ & \leq \left\| \sqrt{n} \left(\boldsymbol{M}_{n}^{-1} - \boldsymbol{I}_{d}^{-1} \right) \right\|_{2} \\ & + \left\| \boldsymbol{M}_{n}^{-1} \right\|_{2}^{2} \left(\left\| \boldsymbol{C}_{n}^{\top} \sqrt{n} (\boldsymbol{D}_{n}^{-1} - \boldsymbol{I}_{d-1}^{-1}) \boldsymbol{C}_{n} \right\|_{2} + \left\| \sqrt{n} (\boldsymbol{C}_{n}^{\top} \boldsymbol{C}_{n} - \boldsymbol{R}_{j,d}^{*}) \right\|_{2} \right) \\ & + \left\| \boldsymbol{N}_{n}^{-1} \boldsymbol{A}_{j,d}^{-1} \boldsymbol{R}_{j,d}^{*} (\boldsymbol{M}_{n}^{-1} - \boldsymbol{I}_{d}^{-1}) \right\|_{2} \\ & \leq \left\| \left\| \sqrt{n} (\boldsymbol{M}_{n}^{-1} - \boldsymbol{I}_{d}^{-1}) \right\|_{2} \\ & \leq \left\| \left\| \sqrt{n} (\boldsymbol{M}_{n}^{-1} - \boldsymbol{I}_{d}^{-1}) \right\|_{2} \\ & + \left\| \boldsymbol{R}_{j,d}^{*} \sqrt{n} (\boldsymbol{M}_{n}^{-1} - \boldsymbol{I}_{d}^{-1}) \right\|_{2} \\ & + \left\| \boldsymbol{M}_{n}^{-1} \right\|_{2}^{2} \left(\left\| \boldsymbol{C}_{n} \right\|_{2}^{2} \left\| \sqrt{n} (\boldsymbol{D}_{n}^{-1} - \boldsymbol{I}_{d-1}^{-1}) \right\|_{2} + \left\| \sqrt{n} (\boldsymbol{C}_{n}^{\top} \boldsymbol{C}_{n} - \boldsymbol{R}_{j,d}^{*}) \right\|_{2} \right) \\ & + \left\| \left\| \boldsymbol{R}_{j,d}^{*} \right\|_{2} \left\| \left| \sqrt{n} (\boldsymbol{M}_{n}^{-1} - \boldsymbol{I}_{d}^{-1}) \right\|_{2} \left\| \boldsymbol{R}_{j,d}^{*} \right\|_{2} \left\| \left| \boldsymbol{M}_{n}^{-1} - \boldsymbol{I}_{d}^{-1} \right| \right\|_{2} + \left\| \sqrt{n} (\boldsymbol{M}_{n}^{-1} - \boldsymbol{I}_{d}^{-1}) \right\|_{2} \left\| \boldsymbol{R}_{j,d}^{*} \right\|_{2} \right) \\ & + \left\| \boldsymbol{R}_{j,d}^{*} \right\|_{2} \left\| \sqrt{n} (\boldsymbol{M}_{n}^{-1} - \boldsymbol{I}_{d}^{-1}) \right\|_{2} \end{aligned}$$

Let us talk about the spectral norms of some of the components of the upper bound of the quantity $\left\|\sqrt{n}\left(\boldsymbol{A}_{j,d}-\boldsymbol{A}_{j,d}^{lim}\right)\right\|_{2}$. As \boldsymbol{M}_{n} converges to \boldsymbol{I}_{d} and matrix inversion and spectral norm are continuous maps on the space of matrices, hence we can say $\left\|\boldsymbol{M}_{n}^{-1}\right\|_{2}^{2} = \mathcal{O}_{P}(1)$. Similarly, we can say the same thing about $\left\|\boldsymbol{C}_{n}\right\|_{2}^{2}$ being tight. Also note that since $\sqrt{n}(\boldsymbol{C}_{n}-\boldsymbol{R}_{j,d})$ has a matrix CLT due to its structure as \boldsymbol{C}_{n} can be written as sum of n iid matrices of dimension $d \times (d-1)$, combined with the fact that $\boldsymbol{A} \mapsto \boldsymbol{A}^{\top}\boldsymbol{A}$ is a continuous map, we can say $\left\|\sqrt{n}(\boldsymbol{C}_{n}^{\top}\boldsymbol{C}_{n}-\boldsymbol{R}_{j,d}^{\top}\boldsymbol{R}_{j,d})\right\|_{2}$ is $\mathcal{O}_{P}(1)$. Also from Equation 18, it is also clear that $\left\|\boldsymbol{R}_{j,d}^{*}\right\|_{2}=1$. The remaining terms of the upper bound can be said to be $\mathcal{O}_{P}(1)$ by using Proposition 1. This completes the proof of the second part of the lemma.

Denoting $\boldsymbol{\alpha}_{x,d} = \left(\alpha_x^{(1)}, \cdots, \alpha_x^{(d)}\right)^{\top}$ and $\boldsymbol{\alpha}_{u,d} = \left(\alpha_u^{(1)}, \cdots, \alpha_u^{(d)}\right)^{\top}$, using Lemma S1.2 and WLLN, we have:

$$\frac{1}{n} \boldsymbol{X}_{n}^{\top} \boldsymbol{H}_{d} = \begin{bmatrix} \frac{1}{n} \boldsymbol{X}_{n}^{\top} \boldsymbol{h}_{n,1} & \cdots & \frac{1}{n} \boldsymbol{X}_{n}^{\top} \boldsymbol{h}_{n,d} \end{bmatrix}_{1 \times d}
\xrightarrow{\frac{P}{n \to \infty}} \begin{bmatrix} \alpha_{x}^{(1)} & \cdots & \alpha_{x}^{(d)} \end{bmatrix} = \boldsymbol{\alpha}_{x,d}^{\top} \tag{21}$$

Similarly, we have:

$$\frac{1}{n} \boldsymbol{U}_n^\top \boldsymbol{H}_d \xrightarrow[n \to \infty]{P} \boldsymbol{\alpha}_{u,d}^\top, \frac{1}{n} \boldsymbol{\epsilon}_n^\top \boldsymbol{H}_d \xrightarrow[n \to \infty]{P} \boldsymbol{0}_d^\top$$

Thus, we have:

$$\hat{\beta}_{-j,n} - \beta = \frac{\frac{1}{n} \boldsymbol{X}_{n}^{\top} \boldsymbol{P}_{d} (\boldsymbol{I}_{n} - \boldsymbol{P}_{-j,d}) \boldsymbol{P}_{d} (\boldsymbol{U}_{n} + \boldsymbol{\epsilon}_{n})}{\frac{1}{n} \boldsymbol{X}_{n}^{\top} \boldsymbol{P}_{d} (\boldsymbol{I}_{n} - \boldsymbol{P}_{-j,d}) \boldsymbol{P}_{d} \boldsymbol{X}_{n}}$$

$$= \frac{\frac{1}{n} \boldsymbol{X}_{n}^{\top} \boldsymbol{H}_{d} \boldsymbol{A}_{j,d} \frac{1}{n} \boldsymbol{H}_{d}^{\top} (\boldsymbol{U}_{n} + \boldsymbol{\epsilon}_{n})}{\frac{1}{n} \boldsymbol{X}_{n}^{\top} \boldsymbol{H}_{d} \boldsymbol{A}_{j,d} \frac{1}{n} \boldsymbol{H}_{d}^{\top} \boldsymbol{X}_{n}}$$

$$\xrightarrow{\boldsymbol{P}} \xrightarrow{\boldsymbol{\alpha}_{x,d}^{\top} \boldsymbol{A}_{j,d}^{lim} (\boldsymbol{\alpha}_{u,d} + \boldsymbol{0}_{d})} = \frac{\alpha_{x}^{(j)} \alpha_{u}^{(j)}}{\alpha_{x}^{(j)^{2}}} = \frac{\alpha_{u}^{(j)}}{\alpha_{x}^{(j)}} = r_{j,d}$$

$$(22)$$

This completes the proof for the consistency of the bias of our drop-one estimator. Next, we will show the asymptotic distribution of the drop one estimator when the index j of the dropped basis function lies in O_X , i.e. $\alpha_u^{(j)} = 0$. Notice that U_n can be decomposed as $U_n = U_{n,d} + (1 - \lambda_d)U_{n,>d}$, where the above condition also means that $U_{n,d} \in \mathscr{C}(H_{-j,d})$. Thus, we have:

$$(\mathbf{I}_n - \mathbf{P}_{-j,d})\mathbf{P}_d\mathbf{U}_n = (1 - \lambda_d)(\mathbf{I}_n - \mathbf{P}_{-j,d})\mathbf{P}_d\mathbf{U}_{n,>d}$$
(23)

Using this, for $j \in O_X$, we can simplify the bias of the estimator as:

$$\hat{\beta}_{-j,n} - \beta$$

$$= \frac{\frac{1}{n} X_{n}^{\top} P_{d}(I_{n} - P_{-j,d}) P_{d}(U_{n} + \epsilon_{n})}{\frac{1}{n} X_{n}^{\top} P_{d}(I_{n} - P_{-j,d}) P_{d} X_{n}}$$

$$= \frac{\frac{1}{n} X_{n}^{\top} P_{d}(I_{n} - P_{-j,d}) P_{d}(U_{n,d} + (1 - \lambda_{d}) U_{n,>d} + \epsilon_{n})}{\frac{1}{n} X_{n}^{\top} P_{d}(I_{n} - P_{-j,d}) P_{d} X_{n}}$$

$$= \frac{\frac{1}{n} X_{n}^{\top} P_{d}(I_{n} - P_{-j,d}) P_{d}((1 - \lambda_{d}) U_{n,>d} + \epsilon_{n})}{\frac{1}{n} X_{n}^{\top} P_{d}(I_{n} - P_{-j,d}) P_{d} X_{n}}$$

$$= \frac{\frac{1}{n} X_{n}^{\top} H_{d} A_{j,d} \frac{1}{n} H_{d}^{\top}((1 - \lambda_{d}) U_{n,>d} + \epsilon_{n})}{\frac{1}{n} X_{n}^{\top} H_{d} A_{j,d} \frac{1}{n} H_{d}^{\top} X_{n}}$$

$$= \underbrace{\frac{1}{n} X_{n}^{\top} H_{d} [A_{j,d}^{lim} + (A_{j,d} - A_{j,d}^{lim})] \frac{1}{n} H_{d}^{\top}((1 - \lambda_{d}) U_{n,>d} + \epsilon_{n})}_{:=L_{n}} \cdot \underbrace{\frac{\alpha_{x,d}^{\top} A_{j,d}^{lim} \alpha_{x,d}}{\frac{1}{n} X_{n}^{\top} H_{d} A_{j,d} \frac{1}{n} H_{d}^{\top} X_{n}}_{:=\zeta_{j,n} \xrightarrow{P} 1}$$

$$(24)$$

Thus, note that the asymptotic distribution of $\sqrt{n} \left(\hat{\beta}_{-j,n} - \beta \right)$ is same as asymptotic distribution of $\sqrt{n} L_n$. Now:

$$\sqrt{n}L_{n} \cdot \boldsymbol{\alpha}_{x,d}^{\top} A_{j,d}^{lim} \boldsymbol{\alpha}_{x,d}$$

$$= \sqrt{n} \frac{1}{n} \boldsymbol{X}_{n}^{\top} \boldsymbol{H}_{d} [A_{j,d}^{lim} + (\boldsymbol{A}_{j,d} - A_{j,d}^{lim})] \frac{1}{n} \boldsymbol{H}_{d}^{\top} ((1 - \lambda_{d}) \boldsymbol{U}_{n,>d} + \boldsymbol{\epsilon}_{n})$$

$$= \sqrt{n} \left[\frac{1}{n} \boldsymbol{X}_{n}^{\top} \boldsymbol{H}_{d} A_{j,d}^{lim} \frac{1}{n} \boldsymbol{H}_{d}^{\top} ((1 - \lambda_{d}) \boldsymbol{U}_{n,>d} + \boldsymbol{\epsilon}_{n}) \right]$$

$$+ \left(\frac{1}{n} \boldsymbol{X}_{n}^{\top} \boldsymbol{H}_{d} \right) \sqrt{n} (\boldsymbol{A}_{j,d} - A_{j,d}^{lim}) \left(\frac{1}{n} \boldsymbol{H}_{d}^{\top} ((1 - \lambda_{d}) \boldsymbol{U}_{n,>d} + \boldsymbol{\epsilon}_{n}) \right)$$

$$\xrightarrow{T_{n}}$$

Next, we show that $T_n = o_P(1)$. In order to see that, notice that from Equation 21 we have, $\frac{1}{n} \boldsymbol{X}_n^{\top} \boldsymbol{H}_d \xrightarrow{P} \boldsymbol{\alpha}_{x,d}$ and thus it is $\mathcal{O}_P(1)$. Also using Lemma S1.2, we can say that $\frac{1}{n} \boldsymbol{H}_d^{\top}((1-\lambda_d)\boldsymbol{U}_{n,>d} + \boldsymbol{\epsilon}_n) \xrightarrow{P} \boldsymbol{0}_d$, Hence we have using Lemma S1.3 that:

$$|T_{n}| = \left| \left(\frac{1}{n} \boldsymbol{X}_{n}^{\top} \boldsymbol{H}_{d} \right) \sqrt{n} (\boldsymbol{A}_{j,d} - \boldsymbol{A}_{j,d}^{lim}) \left(\frac{1}{n} \boldsymbol{H}_{d}^{\top} ((1 - \lambda_{d}) \boldsymbol{U}_{n,>d} + \boldsymbol{\epsilon}_{n}) \right) \right|$$

$$\leq \underbrace{\left\| \frac{1}{n} \boldsymbol{X}_{n}^{\top} \boldsymbol{H}_{d} \right\|_{2}}_{\mathcal{O}_{P}(1)} \underbrace{\left\| \sqrt{n} (\boldsymbol{A}_{j,d} - \boldsymbol{A}_{j,d}^{lim}) \right\|_{2}}_{\mathcal{O}_{P}(1)} \underbrace{\left\| \frac{1}{n} \boldsymbol{H}_{d}^{\top} ((1 - \lambda_{d}) \boldsymbol{U}_{n,>d} + \boldsymbol{\epsilon}_{n}) \right\|_{2}}_{o_{P}(1)}$$

$$= o_{P}(1)$$

Thus, we can say that $\sqrt{n} \left(\hat{\beta}_{-j,n} - \beta \right)$ has the same asymptotic distribution as that of the quantity $\sqrt{n}L_n = R_n \left(\boldsymbol{\alpha}_{x,d}^{\top} A_{j,d}^{lim} \boldsymbol{\alpha}_{x,d} \right)^{-1}$. So let us start deriving the asymptotic distribution of R_n . For that, first let us denote the vector $\boldsymbol{h}_{d,i} = (h_1(S_i), \dots, h_d(S_i))^{\top}$. Hence we can write down R_n as:

$$R_{n} = \sqrt{n} \left[\frac{1}{n} \boldsymbol{X}_{n}^{\top} \boldsymbol{H}_{d} A_{j,d}^{lim} \frac{1}{n} \boldsymbol{H}_{d}^{\top} ((1 - \lambda_{d}) \boldsymbol{U}_{n,>d} + \boldsymbol{\epsilon}_{n}) \right]$$

$$= \sqrt{n} \left[\frac{1}{n} \boldsymbol{X}_{n}^{\top} \boldsymbol{h}_{n,j} \frac{1}{n} \boldsymbol{h}_{n,j}^{\top} ((1 - \lambda_{d}) \boldsymbol{U}_{n,>d} + \boldsymbol{\epsilon}_{n}) \right]$$

$$= \sqrt{n} \left[\underbrace{\left(\frac{1}{n} \sum_{i=1}^{n} X_{i} h_{j}(S_{i}) \right)}_{R_{1,n}} \underbrace{\left(\frac{1}{n} \sum_{i=1}^{n} ((1 - \lambda_{d}) \boldsymbol{U}_{>d,i} + \boldsymbol{\epsilon}_{i}) h_{j}(S_{i}) \right)}_{R_{2,n}} \right]$$

$$= \sqrt{n} R_{1,n} \cdot R_{2,n}$$

$$(25)$$

Let us define $\mathbf{Z}_i = \begin{bmatrix} Z_{i1} \coloneqq X_i h_j(S_i) \\ Z_{i2} \coloneqq ((1 - \lambda_d) U_{>d,i} + \epsilon_i) h_j(S_i) \end{bmatrix}$ which implies $\frac{1}{n} \sum_{i=1}^n \mathbf{Z}_i = \begin{bmatrix} R_{1,n} \\ R_{2,n} \end{bmatrix}$.

First, we will derive a CLT for \mathbf{Z}_i 's as they are iid and then use the Delta Method on the sample averages of \mathbf{Z}_i to get the CLT for R_n . Let us first derive the mean vector $\boldsymbol{\mu}_Z$ for \mathbf{Z}_i . Remember that $\epsilon_i \perp S_i$. Hence $\mathbb{E}X_i h_j(S_i) = \alpha_x^{(j)}$ and $\mathbb{E}((1-\lambda_d)U_{>d,i}+\epsilon_i)h_j(S_i) = 0$ which implies that $\boldsymbol{\mu}_Z^{\top} = \begin{bmatrix} \alpha_x^{(j)} & 0 \end{bmatrix}$. Now, let us look at the covariance matrix of \mathbf{Z}_i denoted by $\mathbf{\Sigma}_Z$. Thus, we have:

$$oldsymbol{\Sigma}_Z = egin{bmatrix} \sigma_1^2 & \sigma_{12} \ \sigma_{12} & \sigma_2^2 \end{bmatrix}$$

For this Delta Method, we will only need σ_2^2 , which we will compute. For that, notice that:

$$\sigma_2^2 = Var((1 - \lambda_d)U_{>d,i} + \epsilon_i)h_j(S_i))$$

$$= \mathbb{E}[(1 - \lambda_d)U_{>d,i} + \epsilon_i)h_j(S_i)]^2$$

$$= (1 - \lambda_d)\mathbb{E}[U_{>d,i}h_j(S_i)]^2 + \sigma_\epsilon^2$$

$$= (1 - \lambda_d)Var[U_{>d,i}h_j(S_i)] + \sigma_\epsilon^2$$

$$:= (1 - \lambda_d)\sigma_{U,j,>d}^2 + \sigma_\epsilon^2$$

Thus, using Multivariate CLT, we can say that:

$$\sqrt{n} \left(\frac{1}{n} \sum_{i=1}^{n} \mathbf{Z}_{i} - \boldsymbol{\mu}_{Z} \right) = \sqrt{n} \left(\begin{bmatrix} R_{1,n} \\ R_{2,n} \end{bmatrix} - \begin{bmatrix} \alpha_{x}^{(j)} \\ 0 \end{bmatrix} \right) \xrightarrow[n \to \infty]{d} \mathcal{N}_{2} \left(\mathbf{0}_{2}, \boldsymbol{\Sigma}_{Z} \right)$$
(26)

Recall from equation 25, we want to get to the CLT for R_n for which we will apply the Delta Method on the CLT that we just derived. For a function $g: \mathbb{R}^2 \to \mathbb{R}$ defined by g(x,y)=xy. The values of the functions g evaluated at μ_Z is given by $g(\mu_Z)=0$. The gradient of the function g is then given by $\nabla g^{\top}=\begin{bmatrix} y & x \end{bmatrix}$. The value of ∇g evaluated at μ_Z is given by $\nabla g^{\top}(\mu_Z)=\begin{bmatrix} 0 & \alpha_x^{(j)} \end{bmatrix}$. This means that:

$$\sigma_R^2 := (\nabla g(\boldsymbol{\mu}_Z))^{\top} \boldsymbol{\Sigma}_Z \nabla g(\boldsymbol{\mu}_Z)$$

$$= \alpha_x^{(j)^2} \sigma_2^2$$

$$= \alpha_x^{(j)^2} (\sigma_{U,j,>d}^2 + \sigma_{\epsilon}^2)$$
(27)

Thus applying Delta Method on the Equation 26, we have:

$$\sqrt{n} \left[g \left(\frac{1}{n} \sum_{i=1}^{n} \mathbf{Z}_{i} \right) - g \left(\boldsymbol{\mu}_{Z} \right) \right] \xrightarrow[n \to \infty]{d} N \left(0, (\nabla g(\boldsymbol{\mu}_{Z}))^{\top} \boldsymbol{\Sigma}_{Z} \nabla g(\boldsymbol{\mu}_{Z}) \right) \\
\Rightarrow \sqrt{n} \left(g \begin{bmatrix} R_{1,n} \\ R_{2,n} \end{bmatrix} - 0 \right) \xrightarrow[n \to \infty]{d} N(0, \sigma_{R}^{2}) \\
\Rightarrow \sqrt{n} \left(R_{1,n} \cdot R_{2,n} \right) \xrightarrow[n \to \infty]{d} N(0, \sigma_{R}^{2}) \\
\Rightarrow R_{n} \xrightarrow[n \to \infty]{d} R \sim N(0, \sigma_{R}^{2}) \quad \text{(see Eqn. 27)}$$

Hence, combining all the components from Equation 24, we have for $j \in O_X$:

$$\sqrt{n} \left(\hat{\beta}_{-j,n} - \beta \right) = \sqrt{n} L_n \zeta_{j,n}$$

$$= \frac{R_n + T_n}{\boldsymbol{\alpha}_{x,d}^{\top} A_{j,d}^{lim} \boldsymbol{\alpha}_{x,d}} \zeta_{j,n}$$

$$= \frac{R_n + T_n}{\alpha_x^{(j)^2}} \zeta_{j,n} \xrightarrow[n \to \infty]{d} \frac{R}{\alpha_x^{(j)^2}} \sim N\left(0, \frac{\sigma_R^2}{\alpha_x^{(j)^4}}\right) = N\left(0, \frac{(1 - \lambda_d)\sigma_{U,j,>d}^2 + \sigma_\epsilon^2}{\alpha_x^{(j)^2}}\right)$$
(29)

This completes the proof on the asymptotic normality of the valid candidates.

Finally, observe that when U has a finite expansion with d basis functions, i.e. when $\lambda_d = 1$, then for $j \in O_X$ recalling that error vector $\boldsymbol{\epsilon}_n$ is independent of the sampled location vector \boldsymbol{S}_n , from Equation 24, we have:

$$\mathbb{E}\left[\hat{\beta}_{-j,n} - \beta\right] = \mathbb{E}_{\boldsymbol{\epsilon}_{n},\boldsymbol{S}_{n}} \left[\frac{\frac{1}{n}\boldsymbol{X}_{n}^{\top}\boldsymbol{H}_{d}\boldsymbol{A}_{j,d}\frac{1}{n}\boldsymbol{H}_{d}^{\top}\boldsymbol{\epsilon}_{n}}{\frac{1}{n}\boldsymbol{X}_{n}^{\top}\boldsymbol{H}_{d}\boldsymbol{A}_{j,d}\frac{1}{n}\boldsymbol{H}_{d}^{\top}\boldsymbol{X}_{n}} \right]$$

$$= \mathbb{E}_{\boldsymbol{S}_{n}} \left[\mathbb{E}\left[\frac{\frac{1}{n}\boldsymbol{X}_{n}^{\top}\boldsymbol{H}_{d}\boldsymbol{A}_{j,d}\frac{1}{n}\boldsymbol{H}_{d}^{\top}\boldsymbol{X}_{n}}{\frac{1}{n}\boldsymbol{X}_{n}^{\top}\boldsymbol{H}_{d}\boldsymbol{A}_{j,d}\frac{1}{n}\boldsymbol{H}_{d}^{\top}\boldsymbol{X}_{n}} \right| \boldsymbol{S}_{n} \right]$$

$$= \mathbb{E}_{\boldsymbol{S}_{n}} \left[\frac{\frac{1}{n}\boldsymbol{X}_{n}^{\top}\boldsymbol{H}_{d}\boldsymbol{A}_{j,d}\frac{1}{n}\boldsymbol{H}_{d}^{\top}\boldsymbol{X}_{n}}{\frac{1}{n}\boldsymbol{X}_{n}^{\top}\boldsymbol{H}_{d}\boldsymbol{A}_{j,d}\frac{1}{n}\boldsymbol{H}_{d}^{\top}\boldsymbol{X}_{n}} \mathbb{E}\left[\boldsymbol{\epsilon}_{n}|\boldsymbol{S}_{n}\right] \right]$$

$$= \mathbb{E}_{\boldsymbol{S}_{n}} \left[\frac{\frac{1}{n}\boldsymbol{X}_{n}^{\top}\boldsymbol{H}_{d}\boldsymbol{A}_{j,d}\frac{1}{n}\boldsymbol{H}_{d}^{\top}\boldsymbol{X}_{n}}{\frac{1}{n}\boldsymbol{H}_{d}^{\top}\boldsymbol{X}_{n}} \mathbb{E}\left[\boldsymbol{\epsilon}_{n}\right] \right]$$

$$= 0$$

$$(30)$$

This proves the finite sample unbiasedness property of our valid drop-one candidate estimator under finite expansion assumption for the unmeasured confounder U. This completes the proof of Theorem 3.

S1.6 Proof of Lemma 2

Proof. To prove this Lemma, we will first state and prove another one, which will be used in the proof.

Lemma S1.4. Let (S, \mathcal{F}, f_S) be a probability space and $\{h_k\}_{k\geq 1} \subset \mathcal{L}^4(\mathcal{D}, f_S)$ an orthonormal system. Fix $d \in \mathbb{N}$. Assume that for each $j \leq d$, the zero set $\{s : h_j(s) = 0\}$ has $f_{S^{-1}}$ measure 0 (equivalently, $h_j^2 > 0$ $f_{S^{-1}}$ -a.e.). For $j \leq d$, set $V_j := \operatorname{span}\{h_k : 1 \leq k \leq d, k \neq j\}$ and define the set $\mathbb{S}_j := \{v \in V_j : ||v||_{f_S} = 1\}$ and $Q_j(v) := \int h_j^2 v^2 f_S$. Then

$$c_* := \inf_{1 \le j \le d} \inf_{v \in \mathbb{S}_j} Q_j(v) > 0.$$

Proof. Step 1 (strict positivity). Fix $j \leq d$ and $v \in V_j \setminus \{0\}$ such that $v \in \mathbb{S}_j$. Then $A := \{s : v(s) \neq 0\}$ has positive f_S -measure. Since $h_j^2 > 0$ f_S -a.e., $B := \{s : h_j(s) \neq 0\}$

has full f_S -measure, and hence $f_S(A \cap B) = f_S(A) > 0$. On $A \cap B$ we have $h_j^2 v^2 > 0$, so

$$Q_j(v) = \int h_j^2 v^2 f_S > 0.$$

Thus Q_j is strictly positive on \mathbb{S}_j .

Step 2 (compactness and continuity under orthonormal bases). Let $\{\phi_1, \ldots, \phi_r\}$ be any orthonormal basis of V_j in $\mathcal{L}^4(\mathcal{D}, f_S)$, where r = d - 1. For $a = (a_1, \ldots, a_r) \in \mathbb{R}^r$ define $T(a) = \sum_{i=1}^r a_i \phi_i$. Because the basis is orthonormal, T is an isometry i.e. $||T(a)||_{f_S} = ||a||_2$. Hence $\mathbb{S}_j = \{T(a) : ||a||_2 = 1\} = T(S^{r-1})$, where $S^{r-1} = \{a \in \mathbb{R}^r : ||a||_2 = 1\}$ is the Euclidean unit sphere. Since S^{r-1} is compact and T is continuous, \mathbb{S}_j is compact. Moreover,

$$Q_j(T(a)) = \sum_{i,k=1}^r a_i a_k \underbrace{\int h_j^2 \phi_i \, \phi_k \, f_S}_{\boldsymbol{G}_{i,k}^{(j)}} = a^{\top} \boldsymbol{G}^{(j)} a,$$

where $G^{(j)}$ is a symmetric $r \times r$ matrix. Thus Q_j is continuous on V_j .

Step 3 (attainment of a strictly positive minimum). By the extreme value theorem, the continuous function Q_j attains a minimum on the compact set \mathbb{S}_j ; denote this minimum by c_j . From Step 1, $Q_j(v) > 0$ for every $v \in \mathbb{S}_j$, so $c_j > 0$. Since there are finitely many indices $1 \leq j \leq d$, set $c_* = \min_{1 \leq j \leq d} c_j > 0$.

Now we can prove Lemma 2, fix $1 \le j \le d$ and assume $\alpha_u^{(j)} = 0$ i.e. $j \in O_X$. Write $R_j := \sum_{k \le d, \, k \ne j} \alpha_u^{(j)} h_k$ and $T := U_{>d}$. Set

$$A_j := \int h_j^2 R_j^2 f_S ds, \qquad B_j := \int h_j^2 T^2 f_S ds, \qquad C_j := \int h_j^2 R_j T f_S ds.$$

Then

$$||h_j U||_{f_S}^2 - ||h_j U_{>d}||_{f_S}^2 = \int h_j^2 (R_j^2 + 2R_j T) f_S ds = A_j + 2C_j.$$

By Cauchy-Schwarz, $|C_j| \leq \sqrt{A_j B_j}$, hence

$$A_j + 2C_j \ge A_j - 2\sqrt{A_j B_j} = \sqrt{A_j} \left(\sqrt{A_j} - 2\sqrt{B_j}\right).$$

We will show that under the assumptions of the lemma, $\sqrt{A_j} > 2\sqrt{B_j}$. First, by Assumption (ii) which ensures $c_* > 0$ (See Lemma S1.4) and $\alpha_u^{(j)} = 0$,

$$A_j = \int h_j^2 R_j^2 f_S ds \ge c_* \|R_j\|_{f_S}^2 = c_* \sum_{k \le d, k \ne j} \alpha_u^{(k)^2} = c_* S_{\text{in}}.$$

Second, by Assumptions (i) and (iii),

$$B_j = \int h_j^2 T^2 f_S ds \le ||h_j||_{\infty}^2 \cdot ||T||_{f_S}^2 \le M^2 \varepsilon.$$

Thus,

$$\sqrt{A_j} \geq \sqrt{c_* S_{\rm in}} > 2\sqrt{M^2 \varepsilon} \geq 2\sqrt{B_j},$$

where the strict inequality is exactly assumption (iii). Therefore $A_j + 2C_j > 0$, i.e., $\|h_j U\|_{f_S}^2 > \|h_j U_{>d}\|_{f_S}^2$.